Pervasive suicidal integrases in deep-sea archaea

Catherine BADEL[1], Violette DA CUNHA[1], Patrick FORTERRE[1,2] & Jacques OBERTO[1*]

[1]Institute for Integrative Biology of the Cell (I2BC), Microbiology Department, CEA, CNRS, Univ. Paris-Sud, Université Paris-Saclay, 91198, Gif-sur-Yvette cedex, France

[2]Institut Pasteur, Unité de Biologie Moléculaire du Gène chez les Extrêmophiles, Département de Microbiologie, 25 rue du Docteur Roux, 75015 Paris, France

* To whom correspondence should be addressed: jacques.oberto@i2bc.paris-saclay.fr

Downloaded from https://academic.oup.com/mbe/advance-article-abstract/doi/10.1093/molbev/msaa041/5739972 by guest on 24 February 2020

© The Author(s) 2020. Published by Oxford University Press on behalf of the Society for Molecular Biology and Evolution. This is an Open Access article distributed under the terms of the Creative Commons Attribution Non-Commercial License (http://creativecommons.org/licenses/by-nc/4.0/), which permits non-commercial re-use, distribution, and reproduction in any medium, provided the original work is properly cited. For commercial re-use, please contact journals.permissions@oup.com

ABSTRACT (247)

Mobile genetic elements often encode integrases which catalyze the site-specific insertion of their genetic information into the host genome and the reverse reaction of excision. Hyperthermophilic archaea harbor integrases belonging to the SSV-family which carry the MGE recombination site within their open reading frame. Upon integration into the host genome, SSV integrases disrupt their own gene into two inactive pseudogenes and are termed suicidal for this reason. The evolutionary maintenance of suicidal integrases, concurring with the high prevalence and multiples recruitments of these recombinases by archaeal MGEs, is highly paradoxical. To elucidate this phenomenon, we analyzed the wide phylogenomic distribution of a prominent class of suicidal integrases which revealed a highly variable integration site specificity. Our results highlighted the remarkable hybrid nature of these enzymes encoded from the assembly of inactive pseudogenes of different origins. The characterization of the biological properties of one of these integrases, $Int^{pT26\text{-}2}$ showed that this enzyme was active over a wide range of temperatures up to 99°C and displayed a less stringent site specificity requirement than comparable integrases. These observations concurred in explaining the pervasiveness of these suicidal integrases in the most hyperthermophilic organisms. The biochemical and phylogenomic data presented here revealed a target site switching system operating on highly thermostable integrases and suggested a new model for split gene reconstitution. By generating fast-evolving pseudogenes at high frequency, suicidal integrases constitute a powerful model to approach the molecular mechanisms involved in the generation of active genes variants by the recombination of proto-genes.

INTRODUCTION

The maintenance and propagation of mobile genetic elements (MGEs) such as plasmids and viruses impose the infection of a suitable cellular host and the deployment of appropriate strategies (Hulter, et al. 2017). Brute force mechanisms such as high copy number grant MGE inheritance into daughter cells after cell division (Million-Weaver and Camps 2014). More refined toxin-antitoxin systems ensure MGE maintenance by relentlessly killing hosts trying to eliminate them (Harms, et al. 2018). These mechanisms prove a burden for the host cells which develop effective countermeasures such as CRISPRs or restriction modification systems (Arber and Dussoix 1962; Hille, et al. 2018). Alternatively, to favor their maintenance, MGEs alleviate their physiological cost for the host (Carroll and Wong 2018). For example, an efficient MGE partitioning allows propagation with a low copy number (Gerdes, et al. 2010; Nordstrom 2006). Some MGEs even carry functions that present an advantage for the host such as resistance genes that increase the fitness of the symbiont in the

Downloaded from https://academic.oup.com/mbe/advance-article-abstract/doi/10.1093/molbev/msaa041/5739972 by guest on 24 February 2020

presence of antibiotics (Carroll and Wong 2018). Contrastingly, particular MGEs have adopted a different potent survival strategy. They have acquired the capacity to integrate their DNA at a particular location of the cellular chromosome without overly altering both genetic programs, using a mechanism known as site-specific recombination (Grindley, et al. 2006; Landy 1989; Landy 2015). By disguising their genome as part of the host chromosome, these MGEs succeed in lowering their negative impact on the host metabolism and in bypassing defense mechanisms. This improved cellular acceptance ensures MGE maintenance and vertical propagation. The reverse reaction of excision regenerates the MGE in its independently replicating form (Gandon 2016) which can infect other host cells. The bi-stable mechanism of site-specific integration/excision is orchestrated by MGE-encoded enzymes belonging to serine- or tyrosine- recombinases (Grindley, et al. 2006). Tyrosine recombinases constitute the most widespread site-specific recombinases and their enzymatic properties have been investigated for decades (Chen, et al. 1992; Guo, et al. 1999; Landy 2015). They typically recognize short identical DNA sequences present simultaneously on the MGE DNA and on its host chromosome. According to the phage Lambda/*Escherichia coli* paradigm, these sequences are termed attB (for attachment Bacteria) and attP (for attachment Phage) (Landy 2015). Integrases catalyze site-specific recombination between these sequences using a timely orchestrated mechanism consisting of two sequentially integrase-generated single-strand cuts in the two att sequences followed by strand-migration and religation (Grindley, et al. 2006). As a result, the exact MGE DNA is integrated into the host chromosome and bordered by attL (for attachment Left) and attR (for attachment Right) sequences which are hybrids of attB and attP. The site-specific recombination between attL and attR, known as excision, regenerates perfectly intact MGE and host chromosomes. The recombination reaction requires in some cases additional protein partners called recombination directionality factors (RDFs) that regulate the orientation of the reaction (Lewis and Hatfull 2001). Interestingly, integrases sharing very similar enzymatic properties have been identified in all domains of life. Bacterial and eukaryotic tyrosine recombinases have been extensively studied (Dorman and Bogue 2016; Jayaram, et al. 2015; Landy 2015; Van Duyne 2015). In contrast, very few archaeal integrases have been fully characterized (Cossu, et al. 2017; Wang, et al. 2018; Zhan, et al. 2015). Archaeal integrases belong to two distinctive types: the SSV type (Type I) and the pNOB8 type (Type II) (She, et al. 2004). The site-specific recombination promoted by Type II enzymes follows the Lambda Int paradigm with separate attP site and integrase gene. Type I is so far restricted to archaea and consists of peculiar suicidal integrases whose attP site resides within the integrase-coding gene (She, et al. 2001). Upon integration, the integrase-coding gene is split into two inactive pseudogenes, int(N) and int(C) on each side of the integrated MGE. Suicidal integrases have been encountered in geothermal environments (Cossu, et al. 2017; She, et al. 2001), the natural habitat of the Euryarchaeal *Thermococcales* comprising one of the most hyperthermophilic organisms (Adam, et al. 2017; Callac, et al. 2016; Schut,

Downloaded from https://academic.oup.com/mbe/advance-article-abstract/doi/10.1093/molbev/msaa041/5739972 by guest on 24 February 2020

et al. 2007). Plasmid pTN3 (Gaudin, et al. 2013) from *Thermococcus nautili* 30-1 (Gorlas, et al. 2014; Oberto, et al. 2014) encodes Int^{pTN3}, the only suicidal integrase that has been characterized in *Thermococcales* so far (Cossu, et al. 2017). This integrase is present in a narrow range of *Thermococcales* and promotes massive genomic inversions in addition to *bona fide* site-specific recombination properties (Cossu, et al. 2017).

The evolutionary maintenance of suicidal integrases, which destroy their own gene, is highly paradoxical and has not been studied so far. In order to elucidate this phenomenon using phylogenomic analyses it was important to identify a larger dataset than the one available for the Int^{pTN3}-like integrases. We recently uncovered a wide geographical distribution among hyperthermophilic archaea of pT26-2 type plasmids encoding suicidal integrases (Badel, et al. 2019). This large plasmid family allowed us to perform robust phylogenies and comparative genomics. The characterization of the enzymatic properties of one of these integrases and the reconstitution of the evolution history of the entire family provided a strong rationale to explain the maintenance and widespread distribution of suicidal integrases in deep-sea archaea using a mechanism involving pseudogenes. If pseudogenes are often described as 'junk DNA', they also provide a source of genetic diversity (Vihinen 2014). In contrast, *de novo* gene birth via transitory proto-genes remains poorly understood (Carvunis, et al. 2012; Siepel 2009). By generating pseudogenes at high frequency, suicidal integrases could constitute a powerful model to investigate the generation of active genes variants by the recombination of proto-genes.

RESULTS

A cluster of related integrases is prevalent in hyperthermophilic Euryarchaea

Plasmid pT26-2 from *Thermococcus* sp.26-2 was the first plasmid isolated from hyperthermophilic Euryarchaea shown to encode a putative integrase, Int^{pT26-2} (Soler, et al. 2010). We wondered whether we would detect Int^{pT26-2} homologs in other hyperthermophilic organisms. A similarity search first performed on the pT26-2 plasmid family (Badel, et al. 2019) and further extended as indicated in Materials and Methods identified 73 integrases constituting Dataset 1 (Table 1). This dataset comprises hyperthermophilic integrases, 54 from *Thermococcales* and 14 from *Archaeoglobales*, and 5 mesophilic integrases from *Methanosarcinales* (Tables 1 and S1). To decipher the evolutionary relationship between these integrases, we built similarity networks including Dataset 1 and all previously known suicidal integrases, using two levels of sensitivity and random walk as detailed in Material and Methods (Fig. 1). The lower similarity threshold assigned all the integrases from Dataset 1 to the same cluster while excluding pTN3-like integrases and SSV-like integrases (Fig.

Downloaded from https://academic.oup.com/mbe/advance-article-abstract/doi/10.1093/molbev/msaa041/5739972 by guest on 24 February 2020

1A). A more stringent similarity threshold applied to Dataset 1 clustered into Dataset 2 most hyperthermophilic integrase from *Thermococcales* and *Archaeoglobales*, constituting Datasets 3 and 4, respectively (Fig. 1B). The integrases of Dataset 2 were present in 30% of closed *Thermococcales* chromosomes (15/51) and in 50% of closed *Archaeoglobales* chromosomes (4/8). Several genomes even contained several copies of these integrases, up to 5 for *Archaeoglobus profundus* DSM5631. Remarkably, we did not detect any multiple or tandem integration events at the same chromosomal site (Table S1). Additionally, the integrases from Dataset 2 originate from organisms with an optimal growth temperature above 75°C (Table S1). The very high prevalence rate of the members of Dataset 2 denoted the extreme pervasiveness of these integrases. This observation prompted us to investigate whether particular biochemical properties of these enzymes could explain their pervasiveness.

Selection of a suicidal integrase and its target sites for biochemical analysis

The majority of the suicidal integrase-coding genes contained in Dataset 2 consists of pseudogenes generated by the insertion of MGE sequences into host chromosomes. Due to the fact that pseudogenes rapidly accumulate deleterious mutations (Liu, et al. 2004), we selected an intact integrase gene encoded by the replicative form of plasmid pT26-2 in *Thermococcus* sp. 26-2 (Soler, et al. 2010). The genomic analysis of the host chromosome revealed the additional presence of an integrated copy of pT26-2. DNA sequence comparison between the plasmid sequence and the extremities of the integrated copy identified the attachment sites of plasmid pT26-2 (Fig. 2A). The attP site corresponded to a portion of the integrase coding gene as expected for suicidal integrases. The chromosomal attachment site (attB) was found in a gene coding for a $tRNA^{Arg}$(TCT). The identification of these sequences allowed us to reconstitute the molecular integration scenario of plasmid pT26-2 into its host chromosome (Fig. 2B).

Int^{pT26-2} can catalyze all three canonical site-specific recombination activities

To investigate the enzymatic properties of this integrase, we over-produced in *Escherichia coli* strep-tagged versions of Int^{pT26-2} and of the Int^{pT26-2}Y327F variant where the catalytic tyrosine is substituted by a phenylalanine. We purified these enzymes and tested their *in vitro* recombination activities using synthetic DNA substrates. We designed the synthetic Int^{pT26-2} recombination site carried by plasmid pCB568 as the entire sequence of the $tRNA^{Arg}$(TCT) gene followed by 6 nucleotides downstream (Fig. 2B). The most straightforward assay to rapidly assert the activity of purified Int^{pT26-2} was an *in vitro* integration reaction. The integrase-catalyzed recombination between identical supercoiled plasmids carrying a single att site was monitored as described previously (Cossu, et al. 2017) through the formation of plasmid dimers and higher-order multimers (Fig. 3A). Int^{pT26-2} was capable of efficiently catalyzing site-specific integration *in vitro*. The capacity of Int^{pT26-2} to promote

Downloaded from https://academic.oup.com/mbe/advance-article-abstract/doi/10.1093/molbev/msaa041/5739972 by guest on 24 February 2020

excision was assayed in a recombination reaction using supercoiled plasmid pCB596 carrying two att sites in direct orientation followed by endonuclease restriction. This excision reaction effectively produced two smaller circular DNA molecules each containing a single att site (Fig. 3B). The substrate and the excised products were easily discriminated via their respective restriction pattern (Fig. 3B). The comparable efficiency of the IntpT26-2-promoted integration and excision suggested that these reactions do not require additional helper proteins contrarily to phage lambda excision and virus SNJ2 integration (Abremski and Gottesman 1981; Wang, et al. 2018). Intra-molecular DNA inversion constituted the third canonical site-specific recombination reaction. We assayed the $Int^{pT26\text{-}2}$ inversion activity on supercoiled plasmid pCB598 containing two att sites in opposite orientations in a recombination reaction followed by endonuclease restriction. In the presence of $Int^{pT26\text{-}2}$, the assay produced the inversion of the sequence delimited by the att sites readily identified by restriction pattern analysis (Fig. 3C). The $Int^{pT26\text{-}2}$Y327F variant was unable to produce detectable site-specific recombination for all three canonical reaction (Fig. 3ABC). The reported activity of several integrases demonstrated a high or mandatory requirement for negatively supercoiled templates (Mizuuchi, et al. 1978; Reed 1981). In hyperthermophilic archaeal cells, the topological state of DNA is still conjectural even if some reports favor a relaxed chromosome (Lopez-Garcia and Forterre 1997). The inversion and integration activities of $Int^{pT26\text{-}2}$ were therefore tested on supercoiled, linear and relaxed DNA templates but no marked preference was observed for a particular topological state (Fig. S1 & S2). All three positive recombination assays demonstrated that $Int^{pT26\text{-}2}$ is a fully functional tyrosine recombinase able to catalyze efficient DNA topology-independent site-specific integration, excision and inversion *in vitro* in the absence of additional co-factors. We then explored other biochemical properties of $Int^{pT26\text{-}2}$ to explain their pervasiveness among hyperthermophilic archaea.

$Int^{pT26\text{-}2}$ att site extremities are not highly stringent

In order to identify the attachment site requirements for positive $Int^{pT26\text{-}2}$ recombination we produced a set of nested deletions starting from a full length $tRNA^{Arg}$ gene followed by 6 additional nucleotides used in the above *in vitro* reactions (Fig. 4). Surprisingly, this test did not provide clear-cut limits for the $Int^{pT26\text{-}2}$ att site. At the 5' end, we observed a progressive reduction in recombination efficiency: the segments L56, L55 and L54 are positive for recombination while sequence L53 is weakly active (Fig. 4D). At the 3' end, a wide range of sequences exhibited a barely detectable gradient of reduced recombination. The observed trend also strongly suggested that the attP site detected *in silico* (L51) is not recombination-proficient *in vitro*. Previously characterized archaeal integrases such as Int^{pTN3} and Int^{SSV2} recognize att sites of different lengths and sequence but always show an abrupt loss of activity when few nucleotides are removed from the shortest recombination-proficient DNA substrate (Cossu, et al. 2017; Zhan, et al. 2015). Contrarily to what was observed previously, it

Downloaded from https://academic.oup.com/mbe/advance-article-abstract/doi/10.1093/molbev/msaa041/5739972 by guest on 24 February 2020

appeared that Int^{pT26-2} retained partial activity over a remarkably wide range of recombination site deletions.

IntpT26-2 is active at near-boiling water temperature

The natural hosts of the pT26-2 plasmid belong to *Thermococcales* which actively grow up to 95°C therefore constituting some of the most hyperthermophilic organisms known to date. The particular distribution of plasmid pT26-2 raised the question whether the recombinase activity of Int^{pT26-2} was optimized for, and restricted to, high temperatures. All *in vitro* Int^{pT26-2} activity assays described above were performed at a near optimal 75°C which constituted the highest documented temperature for *in vitro* site-specific recombination. The optimal reported temperature for other hyperthermophilic recombinases never exceeded 65°C (Cortez, et al. 2010; Cossu, et al. 2017; Zhan, et al. 2015). It was therefore of great interest to test whether the Int^{pT26-2} integrase would catalyze recombination reactions at yet higher temperatures. We performed the inversion assay described in Figure 3C across a wide range of incubation temperatures, from 60°C to 99°C (Fig. 5). Interestingly, Int^{pT26-2} was able to efficiently catalyze site-specific recombination over the whole temperature range while the maximal amount of recombination product was obtained between 75°C and 80°C (Fig. 5A). Temperature-dependent DNA degradation was accounted for in the reaction (Fig. 5B). Remarkably, the inversion product was still observed at 99°C, which was the highest temperature we could assay at atmospheric pressure and constituted the highest reported temperature for the activity of a tyrosine recombinase.

Limited choice of integrases among highly variable hyperthermophilic MGEs

In order to correlate the particular properties of Int^{pT26-2} with their widespread presence among hyperthermophilic archaea, we first analyzed the MGEs from which they originate by comparative genomics. The more stringent network analysis clearly restricted the distribution of Int^{pT26-2} homologs from Dataset 2 to hyperthermophilic Euryarchaeota. We uncovered a total of 47 different MGEs, most of them being integrated elements except virus TPV1 (Gorlas, et al. 2012), plasmids pT26-2 (Soler, et al. 2010) pGE2 (Badel, et al. 2019) and pIRI06c from *Thermococcus* IRI06c (D. Courtine, pers. comm.). These MGEs were highly variable in size, from 8 to 38 kb and in genetic content. Based on their genetic content (see Material and Methods), these MGEs could be ranked in 4 families related to plasmid pT26-2 (25/47), plasmid pAMT11 or TKV1 (8/47) (Gonnet, et al. 2011), fuselloviruses encoding the same major capsid protein (8/47) (Krupovic, et al. 2014) or without known relative (6/47) (Table S1, Fig. S3). Overall, a wide range of different elements, plasmids and viruses, recruited integrases from Dataset 2 further underlining the pervasiveness of these recombinases.

Downloaded from https://academic.oup.com/mbe/advance-article-abstract/doi/10.1093/molbev/msaa041/5739972 by guest on 24 February 2020

Assessing the diversity of Int$^{pT26\text{-}2}$-related hyperthermophilic suicidal integrases and their targets

To investigate the relationships between the more closely related integrases of Dataset 2, we built a phylogenetic tree (Fig. 6). Based on the network analysis results presented in Figure 1, we rooted the tree between the *Thermococcales* integrases (Dataset 3) and the 8 *Archaeoglobales* integrases from Dataset 4. The distal branches of *Thermococcales* were well resolved even if *Archaeoglobales* and basal *Thermococcales* were poorly supported. *Archaeoglobales* integrases displayed long branches in the phylogenetic tree which did not permit us to infer evolutionary relationships (Fig. 6). The *Thermococcales* integrases of Dataset 3 presented a mixture of closely related and divergent enzymes providing the opportunity to study integrase evolution at different scales. To assess more precisely the evolution history of these enzymes, we superimposed over the integrase phylogeny their respective chromosomal integration site and their MGE family as defined above (Fig. 6).

The sequences of the attB and attP target sites were identified as the direct DNA repeats bordering integrated elements (attL & attR) or by comparing episomal MGEs with their host chromosome. The attachment sites of all integrases from Dataset 1 consisted of the 3' end of various tRNA genes without supplementary loop. As a notable exception, the integrases from the *Archaeoglobales* elements AprDSM5631_IE2 and AveSNP6_IE2 recombined att sites with a supplementary loop while element AveSNP6_IE1 recombined at the 5' end of its tRNA gene target (Fig. S4). The 54 *Thermococcales* integrases from Dataset 3 used 14 different tRNA genes for integration whereas the 14 *Archaeoglobales* integrases from Dataset 4 used 9 different tRNA genes reflecting a flexible integration specificity (Table S1). All tRNA without supplementary loop of a given organism such as *Thermococcus kodakarensis*, displayed a more conserved sequence downstream of the anticodon (73% mean pairwise similarity) than upstream (63%) (Datafile 2AB). All att sites of the *Thermococcales* integrases of Dataset 3 shared 75% mean pairwise identity (Datafile 2C) while a portion of the 3' region, the T stem-loop, was even more conserved, at 90% (Datafile 2D). In *T. kodakarensis*, all T stem-loops shared 85% similarity (Datafile 2G).

It is to be noted that for a given integrated element, the attL and attR sequences might differ. We evidenced one such case of non-specific integration with the *Thermococcales* element TspEXT12c_IV1 integrating in a tRNA^{Arg}(CGC) gene (Fig. S5). The attL and attR sequences of this element presented a single A-G nucleotide mismatch at the tip of the tRNA T loop (Fig. S6A-C). Both the A and G alleles were found for tRNA^{Arg}(CGC) in *Thermococcales* (Datafile 3) therefore ruling out sequencing errors or random mutations. Strikingly, the sequences corresponding to attL and attR were also present in the tRNA^{Arg}(TCG) gene of *Thermococcales* (Datafile 3).

Downloaded from https://academic.oup.com/mbe/advance-article-abstract/doi/10.1093/molbev/msaa041/5739972 by guest on 24 February 2020

Differential evolution history of the N- and C-terminal of suicidal integrases and their targets.

Suicidal integrases share as common characteristic to use part of their own gene as attP integration site. The integrase protein sequence at the junction between the Int(N) and Int(C) moieties therefore corresponds to the translation of the att site (Fig. 1). The phylogenetic analysis presented in Figure 6 showed that, as a general rule, closely related integrases targeted the same tRNA gene for integration. In a number of cases however, cognate integrases appeared to have switched specificity resulting in a substantial modification of their amino-acid sequence. In order to understand this phenomenon, we subdivided each integrase gene from Dataset 3 into three parts: 5'-end, attP and 3'-end and compared them and their respective translation to the other members of the dataset. The results revealed 5 different patterns of unusual sequence conservation both at the DNA and protein level (Fig. 7 and S6). The first case demonstrated the acquisition of different att sites, the tRNAVal(CAC) and tRNATyr(GTA) genes respectively, by the distantly related integrases of TKV1 and TthOGL-20P_IP1. These target sites were very likely acquired via two independent events (Fig. 7A & Fig. S6AB). The second case illustrated the recruitment of an identical tRNAVal(TAC) att site by the two phylogenetically distant integrases from Tsp_IP1 and TEXT15c_IE1 (Fig. 7 & Fig. 8B). The two att sites exhibited different lengths and three nucleotide mismatches giving rise to a different protein sequence in the corresponding segment (Fig. S6CD). The att site similarity presumably constituted a convergence due to the limited pool size of the possible tRNA genes for integration rather than a character inherited from their common ancestor, explaining the variation in att site size and translation. In the third case, the closely related integrases of pT26-2 and TGV1 shared the same specificity for a tRNAArg(TCT) gene (Fig. 7C & Fig. S6EF). These proteins exhibited high amino-acid similarity (>70%) (Fig. 7C) as reflected by their proximity in the phylogenetic analysis (Fig. 6). On the other hand, the amino-acid sequences corresponding to their respective att site were strikingly different. This difference was caused by two translation frameshifts occurring immediately upstream and downstream the att site, accounting also for a slight difference in site length (Fig. S6EF). Surprisingly, in its phylogenetic clade, the IntpT26-2 integrase was the only one exhibiting these frameshifts therefore suggesting a single att site acquisition for all clade members followed by a unique shifting event for one member. A similar situation of frameshifting was observed in a fourth case for the integrases of PIRI42c_IE1 and TE10P11_IP1 even if it resulted in similar glycine and proline-rich sequences due to the high GC content of the att site (Fig. 7D & Fig. S6GH). Notably, these proteins and their respective gene exhibited differential sequence conservation upstream and downstream the att region, suggesting a hybrid origin for the two moieties. The fifth case also illustrated the recombinant nature of these enzymes. Integrases originating from two different phylogenetic clades and carried by TE15P30_IV1 and TpiCDGS_IP1 opted for att sites in the related $tRNA^{Gly}$(CCC) and $tRNA^{Gly}$(TTC) genes (Fig. 7E & Fig. S6IJ). Contrarily to other integration events, the *in silico* reconstituted integrase genes of TpiCDGS_IP1

Downloaded from https://academic.oup.com/mbe/advance-article-abstract/doi/10.1093/molbev/msaa041/5739972 by guest on 24 February 2020

carried a frameshift mutation due to a missing nucleotide in the attachment site. The presence of this mutation was confirmed by sequence read mapping of the *T. piezophilus* CDGS genome (kindly provided by the original authors) (Dalmasso, et al. 2016). This situation constituted the exact converse of the differential sequence conservation upstream and downstream the att region observed in the fourth case. The integration of TpiCDGS_IP1 in *Thermococcus piezophilus* CDGS further exposed the recombination mechanism involved in the evolution of suicidal integrases.

Taken together with our *in vitro* data demonstrating $Int^{pT26\text{-}2}$ relaxed target recognition, the succession of cases presented here suggested the presence of an efficient mechanisms for the evolution and specificity switch of suicidal integrases.

DISCUSSION

Suicidal integrases carry their attP DNA recombination site within their own coding sequence. The site-specific recombination reaction with a compatible attP target on the host chromosome causes the disruption -or suicide- of the integrase gene into two inactive stumps. These pseudogenes cannot produce active integrase and therefore prevent MGE excision. Intuitively, episomal MGEs encoding such suicidal integrases would become irreversibly bound to their host genome, incapable of producing further rounds of infection and eventually disappear. Strikingly, we observed recently that the pT26-2 plasmid family encoding such integrases was worldwide distributed and pervaded archaeal populations both as freely replicative plasmids or integrated elements (Badel, et al. 2019). We were interested in solving this apparent paradox using complementary approaches using phylogenomics and *in vitro* enzyme characterization. We examined if the particular *in vitro* recombination properties of one of these enzymes could convey some form of selective advantage to the MGE or its host and provide clues for the evolutionary success of these suicidal integrases.

Suicidal integrases are active at boiling water temperature and present relaxed integration site specificities

We have selected $Int^{pT26\text{-}2}$, the prominent integrase from Dataset 2 to conduct a series of *in vitro* recombination tests. Our results indicated that this enzyme could outstandingly catalyze all the canonical reactions involved in site-specific recombination over a wide range of temperatures up to 99°C (Figs 3 & 5). We reported previously the *in vitro* characterization of Int^{pTN3}, the first integrase isolated from *Thermococcales* and capable of catalyzing site-specific recombinations as well as low sequence specificity recombination reactions with the same outcome as homologous recombination events (Cossu, et al. 2017). Here, we showed that $Int^{pT26\text{-}2}$ did not carry the additional subdomains found in Int^{pTN3} and performed exclusively site-specific recombination reactions. Additional

Downloaded from https://academic.oup.com/mbe/advance-article-abstract/doi/10.1093/molbev/msaa041/5739972 by guest on 24 February 2020

hyperthermophilic site-specific recombinases have been characterized and their activity was assayed *in vitro* at a maximal temperature never exceeding 65°C (Cossu, et al. 2017; Jo, et al. 2017; Serre, et al. 2002; Zhan, et al. 2015). Additionally, these enzymes encoded by self-replicating mobile elements infect hosts with optimal growth temperatures of 85°C at the most. On the other end, the integrases from the Dataset 2 are encoded by MGEs infecting hosts with much higher optimal growth temperatures, up to 105°C as reported for *Pyrococcus kukulkanii* NCB100 (Callac, et al. 2016). Integrases such as Int$^{pT26\text{-}2}$ are therefore particularly well suited to efficiently catalyze integration and spread in environments with a wide range of temperature, including extreme hyperthermophilic conditions.

The integration module conveyed by suicidal integrases is much simpler than what is found in most MGEs. The integration module of bacteriophage Lambda is composed of the integrase gene, a separate att site and additional genes encoding recombination directionality factors (RDFs) to avoid spontaneous MGE excision (Landy 2015). In contrast, the suicidal Int^{pTN3} and Int^{SSV2} integrases were shown to promote *in vitro* excision without recombination directionality factors (Cossu, et al. 2017; Zhan, et al. 2015), the disruption of their gene upon integration acting as directionality regulator. This property was also confirmed for Int$^{pT26\text{-}2}$, which was able to perform both *in vitro* integration and excision reactions with comparable efficiencies (Fig. 3). The compactness of an integration module not requiring RDFs and carrying attP imbedded in the integrase gene constituted very likely a strong advantage to explain the pervasiveness of suicidal integrases among related organisms.

The *in vitro* characterization of Int$^{pT26\text{-}2}$ revealed an additional peculiar property of this integrase regarding its target site. The reported recombination activity of other archaeal integrases such as Int^{pTN3} and Int^{SSV2} was impaired as soon as very few nucleotides were removed from their target substrate (Cossu, et al. 2017; Zhan, et al. 2015). By assaying the recombination activity of Int$^{pT26\text{-}2}$ on nested deletions of attB, we observed that the requirements for a specific site were far less stringent. This integrase was active over a wide range of site deletions as long as the core site was present. In these experiments, the last 10 nucleotides present in both attB and attP and corresponding to the arm sequence were not crucial to allow site-specific recombination (Fig. 4). These observations suggested that recombinases promiscuous in site selection could target various tRNA gene locations of the same genome or even different related hosts. The high occurrence of this type of integrase in Dataset 1 suggested a selective advantage of mobile elements carrying such a promiscuous integrase. A pertinent phylogenomic analysis confirmed these observations for the entire Int$^{pT26\text{-}2}$ integrase dataset.

Integrases from Dataset 1 showed the capacity to target a high variety of sites on the host chromosome namely 18 out of the 46 possible tRNA genes, either at the 5’ or at the 3’ end (Fig. S5).

Downloaded from https://academic.oup.com/mbe/advance-article-abstract/doi/10.1093/molbev/msaa041/5739972 by guest on 24 February 2020

These attachment sites consisted for the vast majority of the 3' end of these tRNA genes, comprising the T stem-loop which is significantly more conserved than the rest of the tRNA with a mean pairwise identity of 90% (Fig. S4 and Datafile 2C). We surmised that this conserved T stem-loop constitutes the core attachment site carrying the cleavage and strand exchange positions of the attB × attP recombination reaction. Outside of this conserved core, the various target sites were more variable both in sequence and length (Datafile 3, Fig. S5). The combination of our phylogenomic analyses with the in vitro activity data presented above strongly suggested that all integrases from Dataset 1 share the intrinsic propensity to easily switch between different att targets with similar core sites.

***Thermococcales* integrases are not species-specific and are frequently exchanged between MGEs**

Our phylogenomic analysis investigated the evolution history of hyperthermophilic suicidal integrases composing Dataset 3 at four different levels. On top of the integrase sequence phylogeny, we superposed their particular target sites and the mobile element of origin (Fig. 6). In addition, we correlated integrases and host species (Table S1). The wide distribution of *Thermococcales* integrases we observed among the various types of elements such as fuselloviruses, pT26-2- or pAMT11-like plasmids and unidentified MGEs can be explained by two evolution histories: (i) the congruence of the phylogenies of the MGES and their associated integrase indicating that theses enzymes diverged from a single common ancestor and co-evolved with the mobile element or (ii) the exchange of integrases between the different MGE types. Strikingly, very similar integrases (94% mean pairwise similarity) were found in the genomes of very distinct mobiles elements: in fuselloviruses (TspEXT12C_IV1 and TAMTc70_IV1), in a pT26-2-like integrated plasmid (TguDSM11113_IP1) and in unidentified integrated elements (T29-3_IE1 and TAMTc94_IE1) (Fig. S7). Such high similarity values indicated a recent exchange of integrase genes between these integrated elements. However, we could not trace the directionality of the transfer due to the lack of bootstrap support. In a similar process, the pAMT11-related plasmid family presumably captured integrases from Dataset 3 at least twice independently, in TpIRI06c_IP1 and TprCol3_IP1 (Fig. 6). Interestingly, the pAMT11 plasmid described originally did not encode an integrase (Gonnet, et al. 2011), suggesting either a corresponding gene loss in this particular plasmid or independent integrase gene acquisitions in the pAMT11-related elements identified in this study. Module exchange between related MGEs is a well-known process (Hendrix, et al. 2000; Iranzo, et al. 2016; Oberto, et al. 1994). In the case of this integrase family, the frequency of genetic exchange or acquisition highlighted the selective advantage provided by $Int^{pT26\text{-}2}$-related integrases to their respective MGE. Additionally, our phylogenetic analysis indicated clearly that the phylogenies of integrases and host chromosomes are not congruent (Fig. 6 and Table S1). *Thermococcales* from distinct genera such as *Thermococcus barophilus* CH5 and *Pyrococcus* sp. NA2 harbored very closely related integrases whereas the distant integrases of elements TKV1, 2 and 3 were found in the same

Downloaded from https://academic.oup.com/mbe/advance-article-abstract/doi/10.1093/molbev/msaa041/5739972 by guest on 24 February 2020

Thermococcus kodakarensis KOD1 isolate. On the other hand, we observed a limited *Pyrococcus* genus specificity for the integrases of pGE2, PkuNCB100_IP1 and PHV1. Overall, the integrases from Dataset 3 seemed to be capable of pervading all *Thermococcales*, without species specificity.

Molecular model for suicidal integrase evolution and target site switching

The Int$^{pT26\text{-}2}$ integrase family allows MGE integration in a variety of chromosomal sites and in a wide range of archaeal organisms belonging to three distinct taxonomic orders. These enzymes are uniquely resilient by efficiently switching target specificity. The comparison of all chromosomal attachment sites demonstrated that these integrases target the 3' end of various tRNA genes which corresponds to their most conserved region. In addition, the *in vitro* activity analysis of Int$^{pT26\text{-}2}$, the most prominent integrase of this dataset clearly showed a relaxed requirement for specific att site extremities. These two properties certainly contributed to the evolution of these enzymes but were not sufficient to explain the extensive target site exchange among closely related integrases (Fig. 6). One would expect that any abrupt att switching would lead to drastic changes in the protein sequence in the att site segment and that these alterations could also extend further downstream due to frameshifting. It can be intuited that in both cases the resulting protein would lose its integrase function. Unexpectedly in Dataset 2, integrase sequences corresponding to the att site diverged either due to different att sequences or to identical att sites translated in alternate frames. In the latter case, we observed frequent site size variation and the presence of indels bordering the att site. These changes, allowing the restoration of a sense reading frame for the C-terminal end of the protein were often found among closely related integrases and were compatible with our biochemical evidence of relaxed sequence requirement at att borders. In addition, the variability of protein sequence encompassing the att site was somewhat constrained by the extensive conservation of the 3' end of the target tRNA genes and its high GC content giving rise to proline- or glycine-rich protein segments. Overall, it appeared clearly that protein sequence changes corresponding to the att site did not affect protein function, making specificity switching easier than anticipated.

The aforementioned results and the thorough genomic comparison of 54 chromosomal integration events from Dataset 1 permitted us to propose a molecular model explaining the prevalence and pervasiveness of suicidal integrases in hyperthermophilic organisms. This model describes the mechanism used for att target switching and is based on successive MGE integrations in the same cellular host. Any integration episode would generate identical attL and attR sequences at its borders while disrupting the suicidal integrase gene (Fig. 1). Each of these att sites can be targeted by the same MGE in a second event of integration to produce a tandem integration reconstituting an intact copy of the integrase gene (Fig. 8A). This particular situation is prone to efficient excision catalyzed by the intact integrase and has not been observed even in the larger Dataset 1 nor for other

Downloaded from https://academic.oup.com/mbe/advance-article-abstract/doi/10.1093/molbev/msaa041/5739972 by guest on 24 February 2020

MGEs carrying suicidal enzymes (Cossu, et al. 2017; Redder, et al. 2009). On the other hand, tandem integration has been observed for MGEs carrying Type II non-suicidal integrases (Krupovic, et al. 2010; Krupovic, et al. 2019) as their excision might be regulated by RDFs. The integration instability of suicidal tandem MGEs could also be used to generate new hybrid suicidal integrases as observed in the case of *Thermococcus piezophilus* TpiCDGS_IP1 (Fig 7E & Fig. S6IJ).

In our model, the tandem integration of two related MGEs carrying divergent integrases followed by homologous recombination releases a hybrid plasmid carrying a potential frameshift in the reconstituted hybrid integrase gene. This event would leave behind a conversely hybrid MGE integrated in the chromosome and presenting two integrase gene moieties of different origin and in different reading frames. We observed this exact situation for the TpiCDGS_IP1 element (Fig. 8B). We have documented additional cases of hybrid integrases displaying separate evolution histories in their Int(N) and Int(C) moieties (Fig. 7DE and Fig. S6GHIJ). Efficient genomic homologous recombination between cognate integrated copies of MGEs was proposed as a mechanisms for the evolution of fuselloviruses in *Sulfolobales* (Redder, et al. 2009), demonstrated more recently by direct sequence analysis in *Thermococcus kodakarensis* as discussed below (Gehring, et al. 2017) and fully supports this model.

An alternative scenario could also account for the generation of hybrid suicidal integrases. Cognate MGEs carrying various integrases from Dataset 2 are often found inserted in different locations of the same host chromosome (Table S1) as shown for other MGEs encoding suicidal integrases (She, et al. 2004; Wang, et al. 2007). Two cognate MGEs integrated in opposite orientations and sharing enough DNA similarity could undergo homologous recombination and generate chromosomal inversions events as reported for the *Thermococcus kodakarensis* TKV2 and TKV3 elements (Gehring, et al. 2017) (Fig. 8C). Such an inversion would bring heterologous attL and attR sites and heterologous integrase moieties into the correct register. A new incoming MGE with a relaxed integrase specificity could excise these recombinant MGEs and generate hybrid integrases with modified target specificities (Fig. 8C).

The simple site specific recombination scheme of suicidal integrase shown in Figure 1 seemed to imply that these enzymes which destroy their own gene would be doomed to disappear by leaving only inactive genes relics. This work demonstrated on the contrary that by integrating, these enzymes generated a fertile bed of fast evolving pseudogenes whose combinations created a wide array of new integrases able to efficiently target 18 different tRNA genes. Our data showed that this variability, a somewhat relaxed target specificity, a very compact integration module devoid of RDFs and an extreme thermostability very likely accounted for the prevalence and unique pervasiveness of this integrase family in hyperthermophilic archaea. It is well accepted that pseudogenes increase the genetic diversity through recombination and gene conversion (Vihinen 2014). In contrast, the

Downloaded from https://academic.oup.com/mbe/advance-article-abstract/doi/10.1093/molbev/msaa041/5739972 by guest on 24 February 2020

emergence in all organisms of new genes via pseudogenes and transitory proto-genes remains poorly understood (Carvunis, et al. 2012; Siepel 2009). By generating pseudogenes and at high frequency, pervasive suicidal integrases could constitute an efficient model to approach the molecular mechanisms involved in the generation of active genes variants by the recombination of proto-genes.

Downloaded from https://academic.oup.com/mbe/advance-article-abstract/doi/10.1093/molbev/msaa041/5739972 by guest on 24 February 2020

MATERIALS AND METHODS

Detection of mobile elements and integrase homologs in Euryarchaea

A classical similarity search in the protein databases to detect proteins closely related to Int^{pT26-2} could not be implemented since SSV-type integrase genes are often mis-annotated due to their fragmentation after integration. Instead, we used tBLASTn with already known and subsequently detected Int(N) and Int(C) moieties as query. As subject sequence, we used the nr/nt nucleotide collection and our own collection of sequenced *Thermococcales* genomes (to be published elsewhere). The detection of genomic integrated elements is a two-step process. In the first step, disrupted integrases and their adjacent att site are located by sequence comparison. We selected hits with an e-value lower than 1e-30 and then reconstituted the complete integrase coding gene. In the second step, the surroundings (<30-40kb) of these locations are scanned for the cognate att direct repeat. This arrangement is unequivocal as tandemly inserted MGEs were never observed. The sequences of integrated MGEs were obtained by extracting from GenBank files DNA segments comprised between attL and attR pairs (Datafile 1). 73 integrases were detected, 20 were already published and 53 were newly identified, including 34 in our genome collection (to be published elsewhere). Mobile elements were assigned to a MGE family based on the presence of marker genes: core genes for the pT26-2 plasmid family (Fig. S3) and the major capsid protein (MCP) gene for the fuselloviruses (Krupovic, et al. 2014). For the pAMT11 plasmid family, no marker gene was previously proposed. We used the three longer genes (ORF1 to 3) conserved between the two previously known members of the family pAMT11 and TKV1 (Gonnet, et al. 2011).

Assessment of integrases relatedness using similarity networks

All-against-all BLASTP analyses were performed on all the integrases comprises in Dataset 1, a set of *Sulfolobales* integrases identified in free Fuselloviridae, and all available pTN3 integrases. The all-against-all integrases BlastP results were grouped using the SiLiX (for *Single Linkage Clustering of Sequences*) package v1.2.8 (http://lbbe.univ-lyon1.fr/SiLiX) (Miele, et al. 2011). This approach for the clustering of homologous sequences is based on single transitive links with alignment coverage

constraints. Several different criteria can be used separately or in combination to infer homology separately (percentage of identity, alignment score or E-value, alignment coverage). For this integrase dataset, the results of the all-against-all BLASTP analyses were filtered with the additional thresholds of BLASTP pairwise similarity >25% or >35% over 60% for the protein (Fig. 1). The network was visualized using the igraph package from R (https://igraph.org/). In order to find densely connected communities in a graph via random walks, we used the cluster_walktrap function of the igraph package.

Thermococcales isolation and sequencing

Thermococcales strains were isolated during the Starmer (1989), Amistad (1999), CIR (2001), Extreme (2001) and Iris (2001) Ifremer campaigns and originate from the Indian Ocean, the Oriental Pacific Ridge and the Mid-Atlantic Ridge (Badel, et al. 2019). DNA sequencing was performed by Genoscope (Centre National de Séquençage, France), using Illumina MiSeq. Reads were assembled with Newbler (release 2.9) and gap closure was performed by PCR, Sanger sequencing and Oxford Nanopore MinION. The sequences of all the integrated elements detected in these isolates are publicly available (Supplemental Datafile 1).

Recombinant protein production and purification

The gene coding for the integrase of plasmid pT26-2 ($Int^{pT26\text{-}2}$, NCBI protein accession YP_003603594.1) was PCR amplified from pT26-2 plasmid DNA with primers pT26-2_F and _R (Table S2). The forward primer added a sequence coding for the Strep-tag at the 5' end of the gene. The PCR product was then assembled with the linearized expression vector pET-26b(+) by Gibson assembly (NEB) and transformed into *Escherichia coli* strain XL1-Blue. The resulting plasmid pCB558 was verified by DNA sequencing. Plasmid pCB616 encoding the variant $Int^{pT26\text{-}2}$Y327F was constructed with the Q5® Site-Directed Mutagenesis Kit (NEB) using the primers pT26-2_Y327F_F and _R (Table S2). *E. coli* Rosetta BL21 (DE3) carrying pCB558 or pCB616 was grown in LB medium to OD 0.5 and recombinant protein production was induced with 250 µM IPTG. $Int^{pT26\text{-}2}$ overproduction in *E. coli* was somewhat toxic. After 1.5 hour induction, cells were harvested and resuspended in the purification buffer (1 M KCl, 40 mM Tris HCl pH 8, 10 % glycerol and 5 mM β-mercaptoethanol) supplemented with a protease inhibitor cocktail (cOmplete™ ULTRA Tablets, EDTA-free, Roche). Cells were lysed by a pressure shock with a one shot cell disruptor (Constant Systems Ltd) and centrifuged at 4°C for 30 min at 18000 g. The supernatant was recovered, heated at 65°C for 10 minutes, centrifuged at 5000 g for 15 min and filtered. The solution was then loaded on a 1 mL StrepTrap HP column (GE Healthcare). The STREP-tagged $Int^{pT26\text{-}2}$ and $Int^{pT26\text{-}2}$Y327F were eluted by the purification buffer supplemented with 2.5 mM d-desthiobiotin. The buffer of $Int^{pT26\text{-}2}$Y327F was depleted in d-desthiobiotin by buffer exchange with a

Downloaded from https://academic.oup.com/mbe/advance-article-abstract/doi/10.1093/molbev/msaa041/5739972 by guest on 24 February 2020

Vivaspin® Centrifugal Concentrators (Sartorius). Int$^{pT26\text{-}2}$ was subsequently loaded on a HiLoad 16/600 75 prep grade column (GE Healthcare) for size exclusion chromatography and fractions containing the protein were concentrated with a Vivaspin® Centrifugal Concentrators (Sartorius). Protein solutions harvested at different steps of the purification were analyzed by SDS-PAGE (Fig. S8). The purified concentrated proteins contained the N-ter strep-tag and their concentration was determined by spectrophotometry.

Integrase substrates construction

To construct plasmid pCB568, we annealed oligonucleotides BamHI-tRNAarg+6-EcoRI_A and _B (Table S2) corresponding to the *T. sp. 26-2* tRNA^{arg} gene and including 6 nucleotides downstream of the gene. The annealing product was digested by EcoRI and BamHI, ligated into a similarly digested pUC18 and transformed into *E. coli* XL1-Blue. The same method was applied for plasmids pCB590, pCB588 and pCB584 with the oligonucleotides BamHI-L56-coRI_A and _B, BamHI-L55-coRI_A and _B and BamHI-L53-coRI_A and _B respectively. Plasmid pCB596 was obtained by Gibson assembly of the following three fragments: (1) pCB568 digested by NdeI, (2) a PCR product amplified from pUC4K with the primers KanR-ex1 and 2 (Table S2) and corresponding to the KmR gene and (3) a PCR product amplified from pCB568 with the primers tRNAarg+6-ex1 and 2 (Table S2) and corresponding to tRNA^{arg} gene and additional 6 nucleotides downstream. The assembled product was transformed into *E. coli* XL1-Blue. The same strategy was used to obtain plasmid pCB598 but with the primers KanR-inv1 and 2 and tRNAarg+6-inv1 and 2 (Table S2) that lead to the assembly of the tRNA^{arg} in the opposite orientation. To obtain plasmids pCB586, pCB602, pCB604, pCB630, pCB632, pCB636 and pCB638, pUC18 was PCR amplified with the forward primer pUC18-H_FOR and the reverse primer L54-pUC18_REV or R49-pUC18_REV or R48-pUC18_REV or R47-pUC18_REV or R46-pUC18_REV or R43-pUC18_REV or R40-pUC18_REV respectively. PCR product was digested by NcoI and HindIII, ligated and transformed into *E. coli* XL1-Blue. All plasmids were verified by DNA sequencing. The plasmids used in this work are listed in Table S3.

Integrase substrates production

Supercoiled plasmids were extracted from *E. coli* XL1-Blue using NucleoSpin Plasmid (Macherey-Nagel) or NucleoBond Xtra Midi (Macherey-Nagel) accordingly to the manufacturer instructions. Relaxed pCB568 and pCB598 were obtained by Nt.BspQI digestion (NEB) followed by a column purification (NucleoSpin Gel and PCR clean-up, Macherey-Nagel). ScaI and PvuII pCB568 fragments were obtained by ScaI and PvuII digestion (FastDigest, ThermoFisher) followed by a gel purification of the desired fragment (NucleoSpin Gel and PCR clean-up, Macherey-Nagel). Linear pCB598 was obtained by ScaI

Downloaded from https://academic.oup.com/mbe/advance-article-abstract/doi/10.1093/molbev/msaa041/5739972 by guest on 24 February 2020

digestion (FastDigest, ThermoFisher) followed by a gel purification (NucleoSpin Gel and PCR clean-up, Macherey-Nagel). A 2106 bp fragment of pCB568 was amplified by Phusion Polymerase (ThermoFisher) with the primers pUC1481-1503 and P30-REV followed by column purification (NucleoSpin Gel and PCR clean-up, Macherey-Nagel). The various fragments of 800 bp were amplified from the appropriate plasmid by Phusion Polymerase (ThermoFisher) with the primers pUC195-217 and pZE21_rev followed by column purification (NucleoSpin Gel and PCR clean-up, Macherey-Nagel).

In vitro integrase enzymatic assay

For *in vitro* enzymatic assays, 500 µg substrate DNA and 200 ng (240 nM) integrase were incubated for 1h at 75°C in 300 mM KCl, 7 mM Tris HCl pH 8, 0.4 % glycerol and 825 µM β-mercaptoethanol in a total volume of 20 µL unless otherwise indicated. In certain cases, two different substrates were mixed in an equimolar ratio for a total mass of 500 µg. For integration assays, reaction product were treated with proteinase K, separated by agarose gel electrophoresis at 50V and subsequently stained with ethidium bromide for visualization. For inversion and excision assays, reaction products were purified with the NucleoSpin Gel and PCR Clean-up kit (Macherey-Nagel), digested with the appropriate restriction enzymes (Fast-digest, ThermoFisher) and separated by gel electrophoresis. Band intensity was quantified with ImageJ (Schneider, et al. 2012) on non-saturated gel pictures using 3 repetitions of the activity assay.

Protein alignment, trimming and phylogenetic analysis.

The alignment used for phylogenetic analyses was performed using MAFFT v7 with default settings (Katoh and Standley 2013) and trimmed with BMGE (Criscuolo and Gribaldo 2010) with a BLOSUM30 matrix, and the -b 1 parameter. IQ-TREE v1.6 (http://www.iqtree.org/) (Nguyen, et al. 2015) was used to calculate maximum likelihood (ML) trees with the best model as suggested by the best model selection option (Kalyaanamoorthy, et al. 2017). Branch robustness was estimated with the nonparametric bootstrap procedure (100 replicates) or with the SH-like approximate likelihood ratio test (Guindon, et al. 2010) and the ultrafast bootstrap approximation (1,000 replicates) (Hoang, et al. 2018). The integrases phylogenetic tree shown in Figure 6 correspond to the tree obtained with the VT+F+I+G4 model on a matrix of 318 positions and with ultrafast bootstrap to indicate the tree robustness. The phylogenetic tree was shaped with the iTOL webtool (Letunic and Bork 2019).

Other bioinformatics analyses

Synteny maps were created using EasyFig (Sullivan, et al. 2011). Pairwise alignments and att site alignments were performed with MUSCLE (Edgar 2004). *Thermococcus kodakarensis* tRNA genes were extracted with GtRNAdb (Chan and Lowe 2016).

Downloaded from https://academic.oup.com/mbe/advance-article-abstract/doi/10.1093/molbev/msaa041/5739972 by guest on 24 February 2020

ACKNOWLEDGEMENTS

The authors wish to thank Dr. Philippe Oger for kindly providing *T. piezophilus* sequencing reads and Dr. Damien Courtine for communicating the sequence of *Thermococcus* IRI06c.

FUNDING

This work was funded by CNRS and the European Research Council under the European Union's Seventh Framework Program (FP/2007-2013)/Project EVOMOBIL - ERC Grant Agreement no. 340440 (PF); Catherine Badel is supported by 'Ecole Normale Supérieure de Lyon'.

REFERENCES

Abremski K, Gottesman S 1981. Site-specific recombination Xis-independent excisive recombination of bacteriophage lambda. J Mol Biol 153: 67-78. doi: 10.1016/0022-2836(81)90527-1

Adam PS, Borrel G, Brochier-Armanet C, Gribaldo S 2017. The growing tree of Archaea: new perspectives on their diversity, evolution and ecology. ISME J 11: 2407-2425. doi: 10.1038/ismej.2017.122

Arber W, Dussoix D 1962. Host specificity of DNA produced by Escherichia coli. I. Host controlled modification of bacteriophage lambda. J Mol Biol 5: 18-36.

Badel C, Erauso G, Gomez AL, Catchpole R, Gonnet M, Oberto J, Forterre P, Da Cunha V 2019. The global distribution and evolutionary history of the pT26-2 archaeal plasmid family. Environ Microbiol. doi: 10.1111/1462-2920.14800

Callac N, Oger P, Lesongeur F, Rattray JE, Vannier P, Michoud G, Beauverger M, Gayet N, Rouxel O, Jebbar M, Godfroy A 2016. Pyrococcus kukulkanii sp. nov., a hyperthermophilic, piezophilic archaeon isolated from a deep-sea hydrothermal vent. Int J Syst Evol Microbiol 66: 3142-3149. doi: 10.1099/ijsem.0.001160

Carroll AC, Wong A 2018. Plasmid persistence: costs, benefits, and the plasmid paradox. Can J Microbiol 64: 293-304. doi: 10.1139/cjm-2017-0609

Carvunis AR, Rolland T, Wapinski I, Calderwood MA, Yildirim MA, Simonis N, Charloteaux B, Hidalgo CA, Barbette J, Santhanam B, Brar GA, Weissman JS, Regev A, Thierry-Mieg N, Cusick ME, Vidal M 2012. Proto-genes and de novo gene birth. Nature 487: 370-374. doi: 10.1038/nature11184

Chan PP, Lowe TM 2016. GtRNAdb 2.0: an expanded database of transfer RNA genes identified in complete and draft genomes. Nucleic Acids Res 44: D184-189. doi: 10.1093/nar/gkv1309

Chen JW, Lee J, Jayaram M 1992. DNA Cleavage in Trans by the Active-Site Tyrosine during Flp Recombination - Switching Protein Partners before Exchanging Strands. Cell 69: 647-658. doi: Doi 10.1016/0092-8674(92)90228-5

Cortez D, Quevillon-Cheruel S, Gribaldo S, Desnoues N, Sezonov G, Forterre P, Serre MC 2010. Evidence for a Xer/dif system for chromosome resolution in archaea. PLoS Genet 6: e1001166. doi: 10.1371/journal.pgen.1001166

Cossu M, Badel C, Catchpole R, Gadelle D, Marguet E, Barbe V, Forterre P, Oberto J 2017. Flipping chromosomes in deep-sea archaea. PLoS Genet 13: e1006847. doi: 10.1371/journal.pgen.1006847

Criscuolo A, Gribaldo S 2010. BMGE (Block Mapping and Gathering with Entropy): a new software for selection of phylogenetic informative regions from multiple sequence alignments. BMC Evol Biol 10: 210. doi: 10.1186/1471-2148-10-210

Downloaded from https://academic.oup.com/mbe/advance-article-abstract/doi/10.1093/molbev/msaa041/5739972 by guest on 24 February 2020

Dalmasso C, Oger P, Courtine D, Georges M, Takai K, Maignien L, Alain K 2016. Complete Genome Sequence of the Hyperthermophilic and Piezophilic Archeon Thermococcus piezophilus CDGST, Able To Grow under Extreme Hydrostatic Pressures. Genome Announc 4. doi: 10.1128/genomeA.00610-16
Dorman CJ, Bogue MM 2016. The interplay between DNA topology and accessory factors in site-specific recombination in bacteria and their bacteriophages. Sci Prog 99: 420-437. doi: 10.3184/003685016X14811202974921
Edgar RC 2004. MUSCLE: multiple sequence alignment with high accuracy and high throughput. Nucleic Acids Res 32: 1792-1797. doi: 10.1093/nar/gkh340
Gandon S 2016. Why Be Temperate: Lessons from Bacteriophage lambda. Trends Microbiol 24: 356-365. doi: 10.1016/j.tim.2016.02.008
Gaudin M, Krupovic M, Marguet E, Gauliard E, Cvirkaite-Krupovic V, Le Cam E, Oberto J, Forterre P 2013. Extracellular membrane vesicles harbouring viral genomes. Environ Microbiol 16: 1167-1175. doi: 10.1111/1462-2920.12235
Gehring AM, Astling DP, Matsumi R, Burkhart BW, Kelman Z, Reeve JN, Jones KL, Santangelo TJ 2017. Genome Replication in Thermococcus kodakarensis Independent of Cdc6 and an Origin of Replication. Front Microbiol 8: 2084. doi: 10.3389/fmicb.2017.02084
Gerdes K, Howard M, Szardenings F 2010. Pushing and pulling in prokaryotic DNA segregation. Cell 141: 927-942. doi: 10.1016/j.cell.2010.05.033
Gonnet M, Erauso G, Prieur D, Le Romancer M 2011. pAMT11, a novel plasmid isolated from a Thermococcus sp. strain closely related to the virus-like integrated element TKV1 of the Thermococcus kodakaraensis genome. Res Microbiol 162: 132-143. doi: 10.1016/j.resmic.2010.11.003
Gorlas A, Croce O, Oberto J, Gauliard E, Forterre P, Marguet E 2014. Thermococcus nautili sp. nov., a hyperthermophilic archaeon isolated from a hydrothermal deep sea vent (East Pacific Ridge). Int J Syst Evol Microbiol 64: 1802-1810. doi: 10.1099/ijs.0.060376-0
Gorlas A, Koonin EV, Bienvenu N, Prieur D, Geslin C 2012. TPV1, the first virus isolated from the hyperthermophilic genus Thermococcus. Environ Microbiol 14: 503-516. doi: 10.1111/j.1462-2920.2011.02662.x
Grindley NDF, Whiteson KL, Rice PA 2006. Mechanisms of site-specific recombination. Annu Rev Biochem 75: 567-605. doi: 10.1146/annurev.biochem.73.011303.073908
Guindon S, Dufayard JF, Lefort V, Anisimova M, Hordijk W, Gascuel O 2010. New algorithms and methods to estimate maximum-likelihood phylogenies: assessing the performance of PhyML 3.0. Syst Biol 59: 307-321. doi: 10.1093/sysbio/syq010
Guo F, Gopaul DN, Van Duyne GD 1999. Asymmetric DNA bending in the Cre-loxP site-specific recombination synapse. Proc Natl Acad Sci U S A 96: 7143-7148.
Harms A, Brodersen DE, Mitarai N, Gerdes K 2018. Toxins, Targets, and Triggers: An Overview of Toxin-Antitoxin Biology. Molecular Cell 70: 768-784. doi: 10.1016/j.molcel.2018.01.003
Hendrix RW, Lawrence JG, Hatfull GF, Casjens S 2000. The origins and ongoing evolution of viruses. Trends Microbiol 8: 504-508.
Hille F, Richter H, Wong SP, Bratovic M, Ressel S, Charpentier E 2018. The Biology of CRISPR-Cas: Backward and Forward. Cell 172: 1239-1259. doi: 10.1016/j.cell.2017.11.032
Hoang DT, Chernomor O, von Haeseler A, Minh BQ, Vinh LS 2018. UFBoot2: Improving the Ultrafast Bootstrap Approximation. Mol Biol Evol 35: 518-522. doi: 10.1093/molbev/msx281
Hulter N, Ilhan J, Wein T, Kadibalban AS, Hammerschmidt K, Dagan T 2017. An evolutionary perspective on plasmid lifestyle modes. Curr Opin Microbiol 38: 74-80. doi: 10.1016/j.mib.2017.05.001
Iranzo J, Koonin EV, Prangishvili D, Krupovic M 2016. Bipartite Network Analysis of the Archaeal Virosphere: Evolutionary Connections between Viruses and Capsidless Mobile Elements. J Virol 90: 11043-11055. doi: 10.1128/JVI.01622-16
Jayaram M, Ma CH, Kachroo AH, Rowley PA, Guga P, Fan HF, Voziyanov Y 2015. An Overview of Tyrosine Site-specific Recombination: From an Flp Perspective. Microbiology spectrum 3. doi: 10.1128/microbiolspec.MDNA3-0021-2014

Downloaded from https://academic.oup.com/mbe/advance-article-abstract/doi/10.1093/molbev/msaa041/5739972 by guest on 24 February 2020

Jo M, Murayama Y, Tsutsui Y, Iwasaki H 2017. In vitro site-specific recombination mediated by the tyrosine recombinase XerA of Thermoplasma acidophilum. Genes Cells 22: 646-661. doi: 10.1111/gtc.12503
Kalyaanamoorthy S, Minh BQ, Wong TKF, von Haeseler A, Jermiin LS 2017. ModelFinder: fast model selection for accurate phylogenetic estimates. Nat Methods 14: 587-589. doi: 10.1038/nmeth.4285
Katoh K, Standley DM 2013. MAFFT multiple sequence alignment software version 7: improvements in performance and usability. Mol Biol Evol 30: 772-780. doi: 10.1093/molbev/mst010
Krupovic M, Forterre P, Bamford DH 2010. Comparative analysis of the mosaic genomes of tailed archaeal viruses and proviruses suggests common themes for virion architecture and assembly with tailed viruses of bacteria. J Mol Biol 397: 144-160. doi: 10.1016/j.jmb.2010.01.037
Krupovic M, Makarova KS, Wolf YI, Medvedeva S, Prangishvili D, Forterre P, Koonin EV 2019. Integrated mobile genetic elements in Thaumarchaeota. Environ Microbiol. doi: 10.1111/1462-2920.14564
Krupovic M, Quemin ER, Bamford DH, Forterre P, Prangishvili D 2014. Unification of the globally distributed spindle-shaped viruses of the archaea. J Virol 88: 2354-2358. doi: 10.1128/JVI.02941-13
Landy A 1989. Dynamic, structural, and regulatory aspects of lambda site-specific recombination. Annu Rev Biochem 58: 913-949. doi: 10.1146/annurev.bi.58.070189.004405
Landy A 2015. The lambda Integrase Site-specific Recombination Pathway. Microbiology spectrum 3: MDNA3-0051-2014.
Letunic I, Bork P 2019. Interactive Tree Of Life (iTOL) v4: recent updates and new developments. Nucleic Acids Res. doi: 10.1093/nar/gkz239
Lewis JA, Hatfull GF 2001. Control of directionality in integrase-mediated recombination: examination of recombination directionality factors (RDFs) including Xis and Cox proteins. Nucleic Acids Res 29: 2205-2216.
Liu Y, Harrison PM, Kunin V, Gerstein M 2004. Comprehensive analysis of pseudogenes in prokaryotes: widespread gene decay and failure of putative horizontally transferred genes. Genome Biol 5: R64. doi: 10.1186/gb-2004-5-9-r64
Lopez-Garcia P, Forterre P 1997. DNA topology in hyperthermophilic archaea: reference states and their variation with growth phase, growth temperature, and temperature stresses. Mol Microbiol 23: 1267-1279.
Miele V, Penel S, Duret L 2011. Ultra-fast sequence clustering from similarity networks with SiLiX. BMC Bioinformatics 12: 116. doi: 10.1186/1471-2105-12-116
Million-Weaver S, Camps M 2014. Mechanisms of plasmid segregation: have multicopy plasmids been overlooked? Plasmid 75: 27-36. doi: 10.1016/j.plasmid.2014.07.002
Mizuuchi K, Gellert M, Nash HA 1978. Involement of supertwisted DNA in integrative recombination of bacteriophage lambda. J Mol Biol 121: 375-392.
Nguyen LT, Schmidt HA, von Haeseler A, Minh BQ 2015. IQ-TREE: a fast and effective stochastic algorithm for estimating maximum-likelihood phylogenies. Mol Biol Evol 32: 268-274. doi: 10.1093/molbev/msu300
Nordstrom K 2006. Plasmid R1--replication and its control. Plasmid 55: 1-26. doi: 10.1016/j.plasmid.2005.07.002
Oberto J, Gaudin M, Cossu M, Gorlas A, Slesarev A, Marguet E, Forterre P 2014. Genome Sequence of a Hyperthermophilic Archaeon, Thermococcus nautili 30-1, That Produces Viral Vesicles. Genome Announc 2: e00243-00214. doi: 10.1128/genomeA.00243-14
Oberto J, Sloan SB, Weisberg RA 1994. A segment of the phage HK022 chromosome is a mosaic of other lambdoid chromosomes. Nucleic Acids Res 22: 354-356.
Redder P, Peng X, Brugger K, Shah SA, Roesch F, Greve B, She Q, Schleper C, Forterre P, Garrett RA, Prangishvili D 2009. Four newly isolated fuselloviruses from extreme geothermal environments reveal unusual morphologies and a possible interviral recombination mechanism. Environ Microbiol 11: 2849-2862. doi: 10.1111/j.1462-2920.2009.02009.x
Reed RR 1981. Transposon-mediated site-specific recombination: a defined in vitro system. Cell 25: 713-719.

Downloaded from https://academic.oup.com/mbe/advance-article-abstract/doi/10.1093/molbev/msaa041/5739972 by guest on 24 February 2020

Schneider CA, Rasband WS, Eliceiri KW 2012. NIH Image to ImageJ: 25 years of image analysis. Nat Methods 9: 671-675.
Schut GJ, Bridger SL, Adams MW 2007. Insights into the metabolism of elemental sulfur by the hyperthermophilic archaeon Pyrococcus furiosus: characterization of a coenzyme A- dependent NAD(P)H sulfur oxidoreductase. J Bacteriol 189: 4431-4441. doi: 10.1128/JB.00031-07
Serre MC, Letzelter C, Garel JR, Duguet M 2002. Cleavage properties of an archaeal site-specific recombinase, the SSV1 integrase. Journal of Biological Chemistry 277: 16758-16767. doi: 10.1074/jbc.M200707200
She Q, Chen B, Chen L 2004. Archaeal integrases and mechanisms of gene capture. Biochem Soc Trans 32: 222-226. doi: Doi 10.1042/Bst0320222
She Q, Peng X, Zillig W, Garrett RA 2001. Gene capture in archaeal chromosomes. Nature 409: 478. doi: 10.1038/35054138
Siepel A 2009. Darwinian alchemy: Human genes from noncoding DNA. Genome Res 19: 1693-1695. doi: 10.1101/gr.098376.109
Soler N, Marguet E, Cortez D, Desnoues N, Keller J, van Tilbeurgh H, Sezonov G, Forterre P 2010. Two novel families of plasmids from hyperthermophilic archaea encoding new families of replication proteins. Nucleic Acids Res 38: 5088-5104. doi: 10.1093/nar/gkq236
Sullivan MJ, Petty NK, Beatson SA 2011. Easyfig: a genome comparison visualizer. Bioinformatics 27: 1009-1010. doi: 10.1093/bioinformatics/btr039
Van Duyne GD 2015. Cre Recombinase. Microbiology spectrum 3: MDNA3-0014-2014. doi: 10.1128/microbiolspec.MDNA3-0014-2014
Vihinen M 2014. Contribution of pseudogenes to sequence diversity. Methods Mol Biol 1167: 15-24. doi: 10.1007/978-1-4939-0835-6_2
Wang J, Liu Y, Liu Y, Du K, Xu S, Wang Y, Krupovic M, Chen X 2018. A novel family of tyrosine integrases encoded by the temperate pleolipovirus SNJ2. Nucleic Acids Res 46: 2521-2536. doi: 10.1093/nar/gky005
Wang Y, Duan Z, Zhu H, Guo X, Wang Z, Zhou J, She Q, Huang L 2007. A novel Sulfolobus non-conjugative extrachromosomal genetic element capable of integration into the host genome and spreading in the presence of a fusellovirus. Virology 363: 124-133. doi: 10.1016/j.virol.2007.01.035
Zhan ZY, Zhou J, Huang L 2015. Site-Specific Recombination by SSV2 Integrase: Substrate Requirement and Domain Functions. J Virol 89: 10934-10944. doi: 10.1128/Jvi.01637-15

TABLE

Table 1. Integrase datasets used in this study.

Integrase dataset	Number of Integrases	Tandem Integration number	Host phyla	Dataset description
1	73	0	*Thermococcales*, *Archaeoglobales* and *Methanosarcinales*	Larger dataset. All suicide integrases clustering with Int$^{pT26\text{-}2}$ in network A (Fig. 1A)
2	62	0	*Thermococcales* and *Archaeoglobales*	Subset of Dataset 1. Clustering integrases in network B (Fig. 1B)
3	54	0	*Thermococcales*	Subset of Dataset 2. *Thermococcales* integrases
4	8	0	*Archaeoglobales*	Subset of Dataset 3.

Downloaded from https://academic.oup.com/mbe/advance-article-abstract/doi/10.1093/molbev/msaa041/5739972 by guest on 24 February 2020

FIGURES LEGENDS

Figure 1. Archaeal suicidal integrases similarity network. All available archaeal suicidal integrases identified as described in Material and Methods were analyzed through a similarity network. Each dot corresponds to a protein. A random walk algorithm was used for protein clustering. For both networks, proteins are colored depending on their clustering as indicated in the boxed legend. The star points to Int^{pT26-2}.The datasets defined in Table 1 are indicated. **A.** Links between two proteins refer to a BLASTP pairwise similarity >25% over 60% of the protein. **B.** Pairwise similarity >35% over 60% of the protein.

Figure 2. Plasmid pT26-2 integration model. A. Alignment of the pT26-2 attP (P) sequence with the attL (L) and attR (R) sequences from *Thermococcus* sp. 26-2. The conserved sequence is the attachment site (att) that corresponds to the 3' end of a tRNA^{Arg}(TCT) gene. The anti-codon sequence is underlined. The attB site starts 2 nucleotides upstream of the anticodon sequence and extends 6 nucleotides downstream of the tRNA gene (dotted line). Thes sequence identity between attP and attB extends over 51bp. The sequences of the integrase and tRNA genes are antiparallel. **B.** Plasmid pT26-2 was present as a freely replicating element and integrated in the chromosome of *Thermococcus* sp. 26-2. The chromosomal attachment site (attB) corresponds to a the tRNA^{Arg}(CTC) gene (in grey). Upon integration, the integrase gene is split in two parts named int(C) and int(N). The catalytic tyrosine residue (*) is located in the int(C) part.

Figure 3. Int^{pT26-2} site-specific recombination assays for the three canonical activities: integration, excision and inversion. The recombination model is presented for each activity assay. **A. Integration.** Recombination between two att sites (triangles) carried by two identical plasmids pCB568 producing plasmid dimers. Plasmid pUC18 without att site cannot undergo site-specific recombination. Plasmids containing zero or one att site were incubated with purified Int^{pT26-2} (WT) or variant Int^{pT26-2}Y327F (YF) at 75°C during 1h or 6h. Samples were treated with proteinase K and separated on agarose gel. The Y recombinase and att site are necessary and sufficient for the integration activity. Wild-type Int^{pT26-2} introduces topoisomers in supercoiled templates devoid of att site such as pUC18. This indicates that IntpT26 2 can perform the first step of recombination, i.e. non-specific single-strand cleavage, followed by re-ligation of the non-specific substrate, leading to the formation of a topoisomer ladder. **B. Excision.** Intramolecular recombination between two att sites in direct orientation leading to the

Downloaded from https://academic.oup.com/mbe/advance-article-abstract/doi/10.1093/molbev/msaa041/5739972 by guest on 24 February 2020

formation of two plasmids (excision) with one att site each. Different ScaI-EcoRI restriction identify substrate and products. Plasmid pCB596 was incubated with WT or YF at 75°C during 2h and digested with ScaI and EcoRI. **C. Inversion.** Intramolecular recombination between two att sites in inverted orientation leads to the inversion of the intervening segment. The substrate and product have different ScaI-XhoI restriction patterns. Plasmid pCB598 was incubated with WT or YF at 75°C during 2h and digested with ScaI and XhoI.

Figure 4. Minimal att recombination site. A. A nested deletion set of $tRNA^{Arg}$(TCT) sequences were tested as substrates for $Int^{pT26\text{-}2}$ recombination. **B.** The leaf-like structure of *T. 26-2* $tRNA^{Arg}$(TCT) is presented. **C.** The set of nested sequences were tested for recombination against a full length $tRNA^{Arg}$(TCT) gene plus 6nt downstream. When recombination occurs, two chimeric linear substrates of intermediate size are produced. **D.** The two linear substrates were incubated with purified $Int^{pT26\text{-}2}$ for 2h at 75°C, treated with proteinase K and run on an agarose gel.

Figure 5. Temperature activity range of $Int^{pT26\text{-}2}$. The inversion assay presented in Figure 3C was used to test the temperature activity range of $Int^{pT26\text{-}2}$. **A.** Plasmid pCB598 was incubated with purified $Int^{pT26\text{-}2}$ at different temperatures during 0.5h and digested with ScaI and XhoI. **B**. Template DNA was decaying probably due to thermal degradation. To take degradation into account, we quantified the substrate/product ratio in 3 replicate experiments which demonstrated an optimal inversion rate between 80°C and 85 °C. Relative amounts of substrate and product were calculated for each lane, in triplicate. The error bar represents a 95% confidence interval. The difference between apparent and real in vitro IntpT26 2 optimal recombination temperatures was therefore due to DNA degradation at the highest temperatures.

Figure 6. Maximum likelihood phylogenic tree of the integrases from Dataset 2. Branch values represent the posterior probability. Branches supported by both the posterior probability and ultrafast bootstrap (>95%) are indicated by a black dot. The integrated element classification is color-indicated indicated when known, see also Table S1. The individual tRNA genes used for integration are indicated as well as their anti-codon sequence. The scale bar represents the average number of substitutions per site.

Figure 7. **Independent evolution of integrases and their target sites**. For suicidal integrases, the att site is located inside the gene coding for the integrase and is therefore translated along with the integrase. Different cases illustrating the independent evolution of the integrases of Dataset 3 and their respective target sites are summarized here. Gene sequences (DNA) or integrase protein

Downloaded from https://academic.oup.com/mbe/advance-article-abstract/doi/10.1093/molbev/msaa041/5739972 by guest on 24 February 2020

sequences (proteins) were aligned. Mean pairwise similarity over the Int(N), att or Int(C) regions is indicated by a color scale. High similarities (>70%) are indicated in dark blue. Lower similarities (<70%) are indicated in light blue. The 70% cutoff was selected because it corresponds to the similarity between the closely related integrases from elements TGV1 and pT26-2. The phylogenetic distance (d) between proteins is calculated in the same units as in Figure 6. **A.** General case: completely divergent integrases at the DNA and protein levels. **B.** Two divergent integrases sharing the same att site but translated in different frames. **C.** The integrases are closely related as indicated by their similar gene and protein sequences. The same att sequence is translated in a different frame. **D.** The two integrases are closely related at their Int(C) as indicated by their similar gene and protein sequences but with divergent Int(N) segments. Similarly to C, the att sequence translation is different between the two proteins, due to a frameshift. **E.** The two integrases are closely related at their Int(N) as indicated by their similar gene and protein sequences but with divergent Int(C) segments. The att site is translated in a different frame. Complete att site and protein alignments are available in Figure S7.

Figure 8. Model for the formation of hybrid integrases. A. Tandem insertion of the same MGE in the same tRNA gene target reconstituting a functional integrase gene able to excise the element. Identical tandem insertions have never been observed. **B.** A first MGE integration event generated an attR site with a single nucleotide deletion as compared to the original $tRNA^{Gly}$ gene (red dot) (Fig. S6 IJ). The second integration event involved a related MGE but with a more distant integrase. This integration generates an inactive integrase gene (red bar) due to frameshifting. Homologous recombination between related MGE backbones could have excised a hybrid plasmid leading to the situation observed for the integrated TpiCDGS_IP1. The Int(N) and Int(C) segments of its integrase have a different evolution history and cannot be assembled due to a mirrored frameshift in the att region. **C.** Multiple MGE integration events at separate chromosomal locations and in inverted orientation can give rise to a large genomic inversion by homologous recombination between related MGE backbones as reported (Gehring, et al. 2017). This inversion generates hybrid MGEs which could excise by the means of a compatible integrase provided *in trans* via superinfection. The asterisk refers to the codon of the catalytic tyrosine. The eye icon indicates whether particular MGE forms were observed and described.

Downloaded from https://academic.oup.com/mbe/advance-article-abstract/doi/10.1093/molbev/msaa041/5739972 by guest on 24 February 2020

Figure 1.

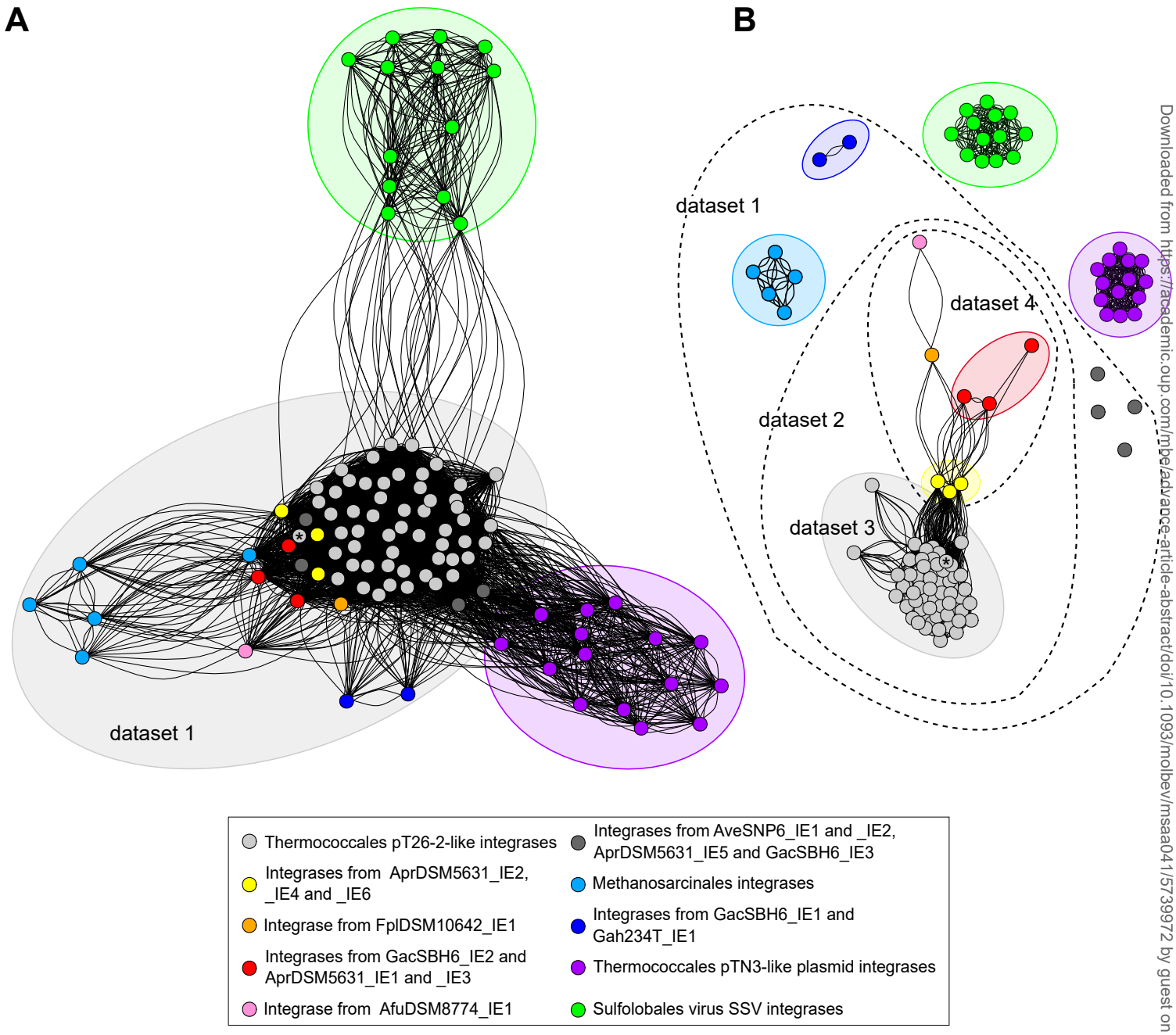

Downloaded from https://academic.oup.com/mbe/advance-article-abstract/doi/10.1093/molbev/msaa041/5739972 by guest on 24 February 2020

Figure 2.

A

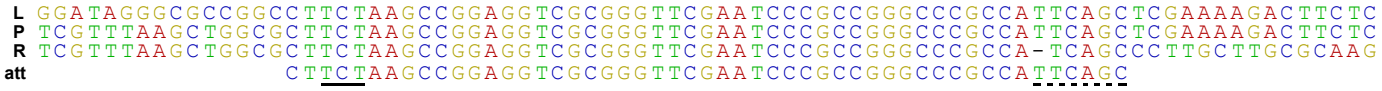

B

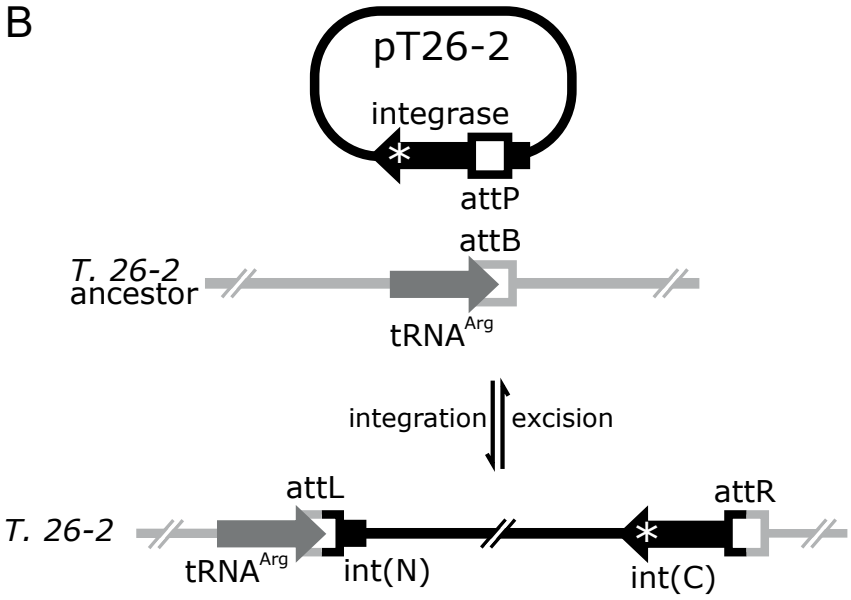

Downloaded from https://academic.oup.com/mbe/advance-article-abstract/doi/10.1093/molbev/msaa041/5739972 by guest on 24 February 2020

Figure 3.

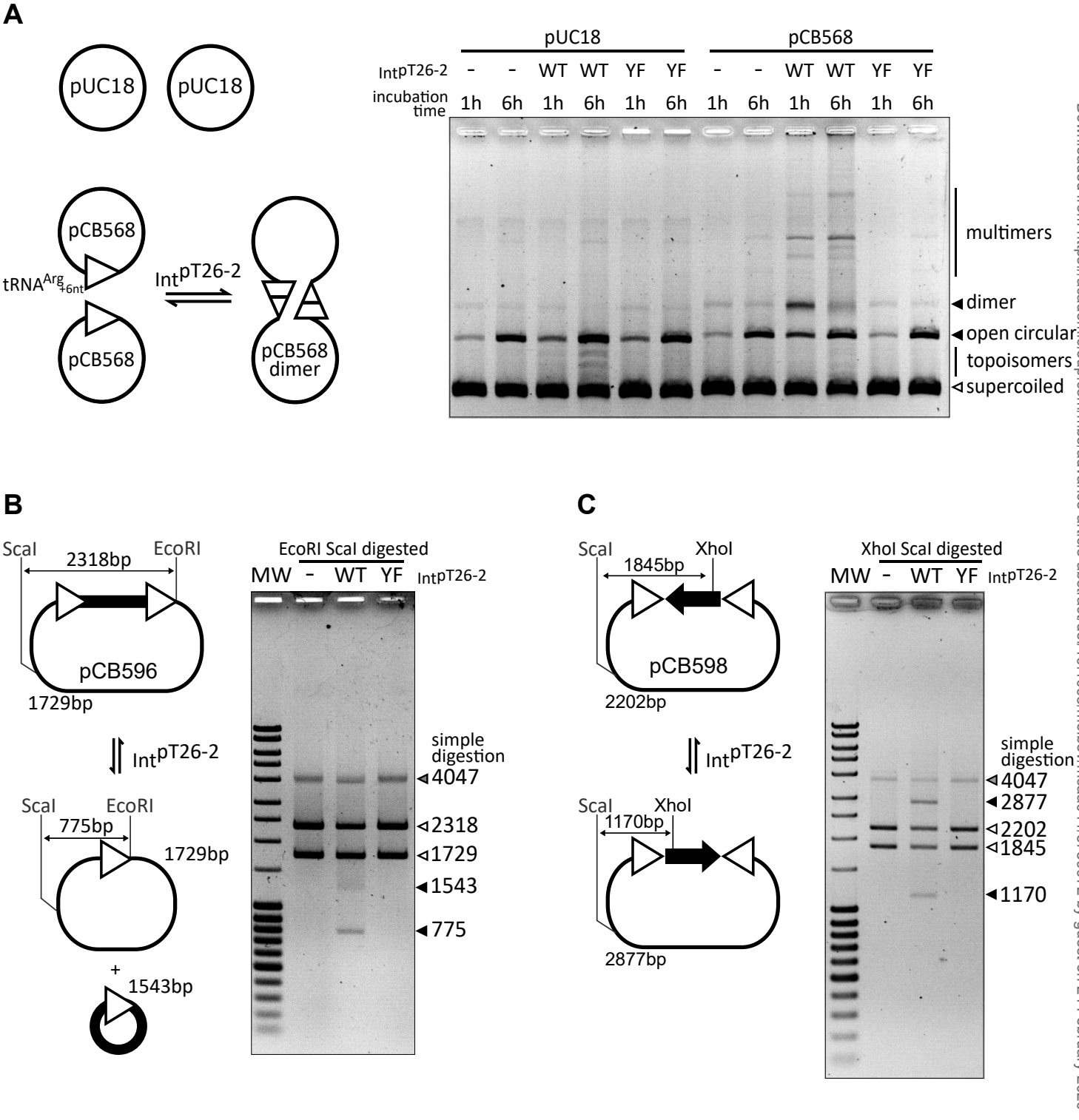

Downloaded from https://academic.oup.com/mbe/advance-article-abstract/doi/10.1093/molbev/msaa041/5739972 by guest on 24 February 2020

Figure 4.

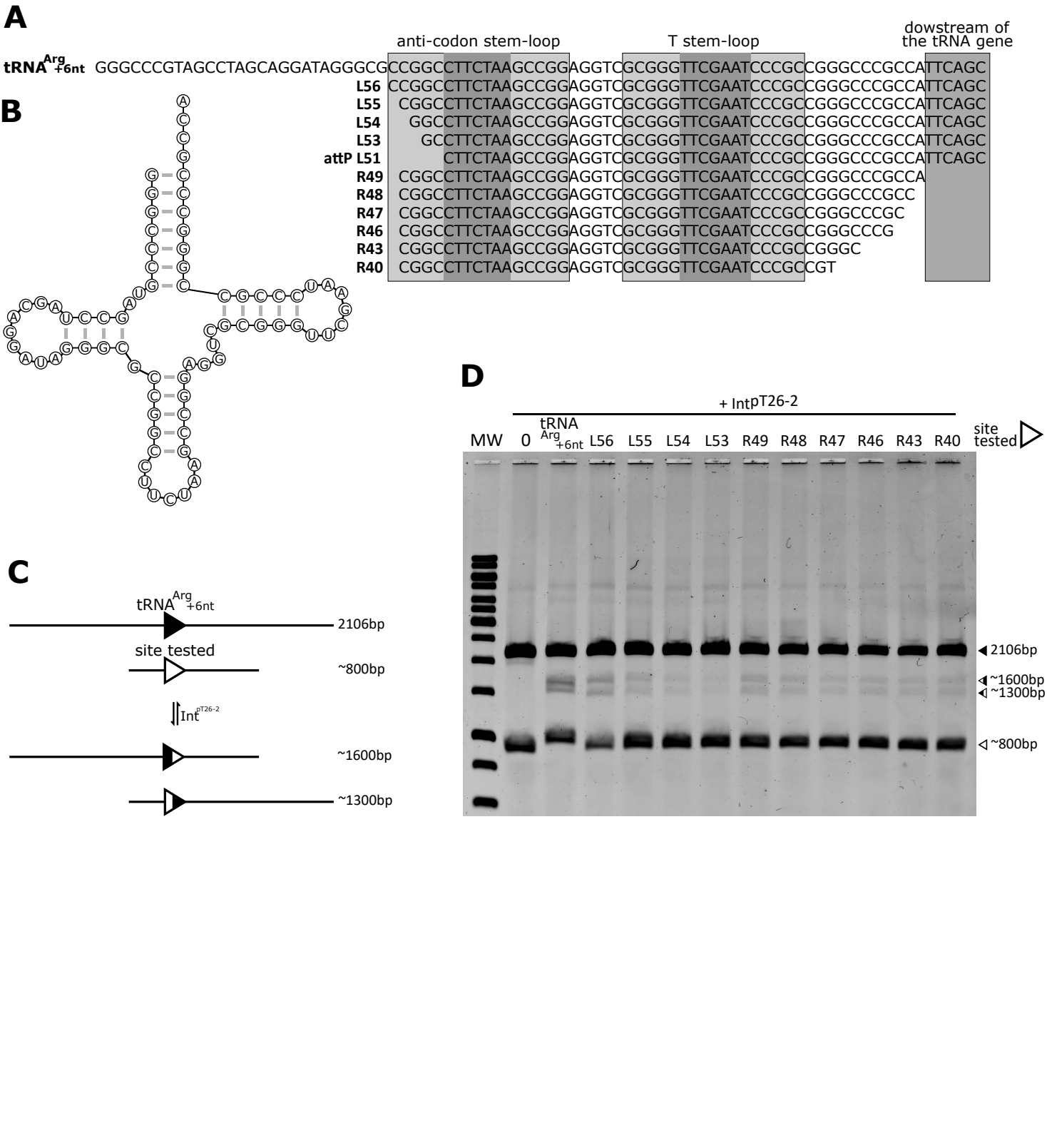

Downloaded from https://academic.oup.com/mbe/advance-article-abstract/doi/10.1093/molbev/msaa041/5739972 by guest on 24 February 2020

Figure 5.

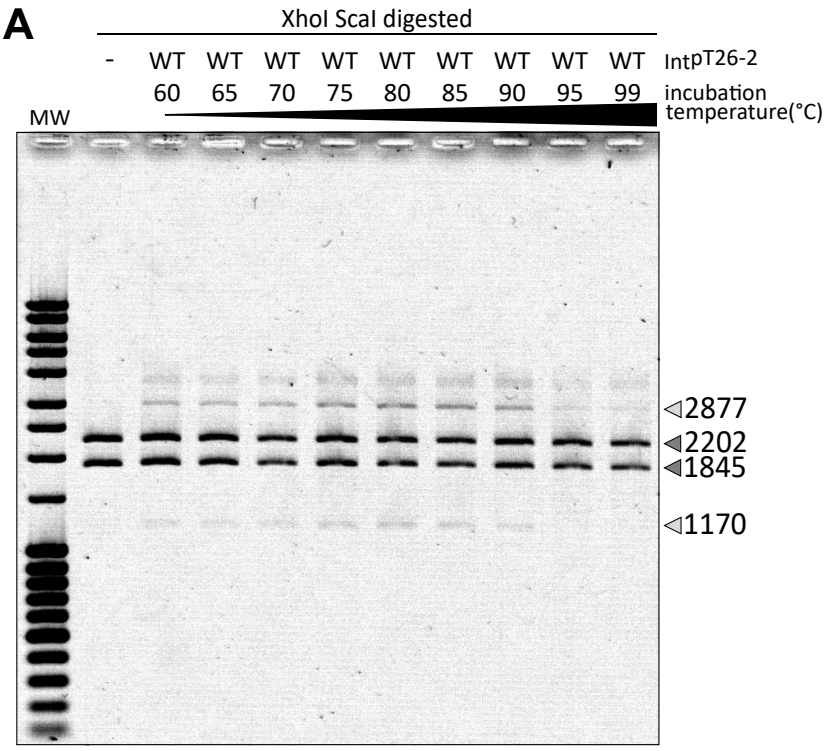

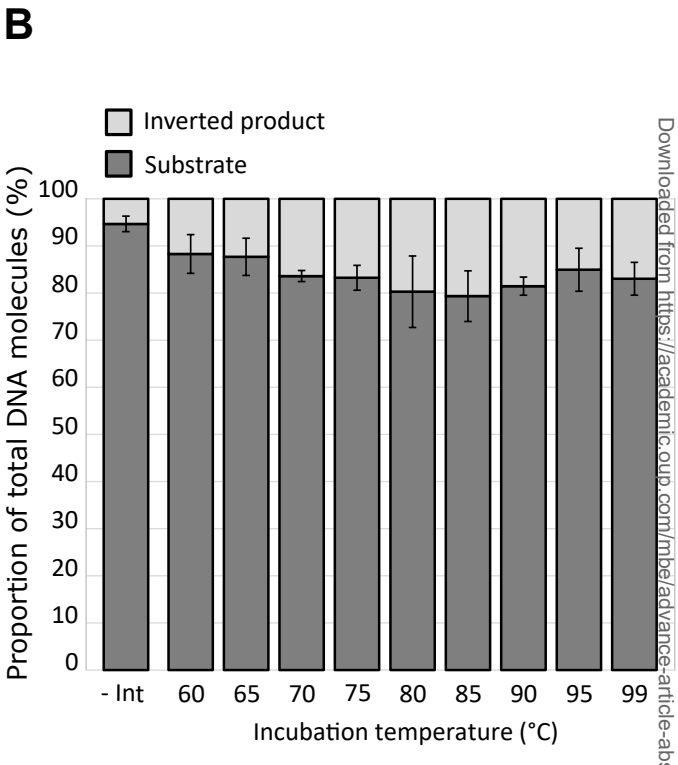

Downloaded from https://academic.oup.com/mbe/advance-article-abstract/doi/10.1093/molbev/msaa041/5739972 by guest on 24 February 2020

Figure 6.

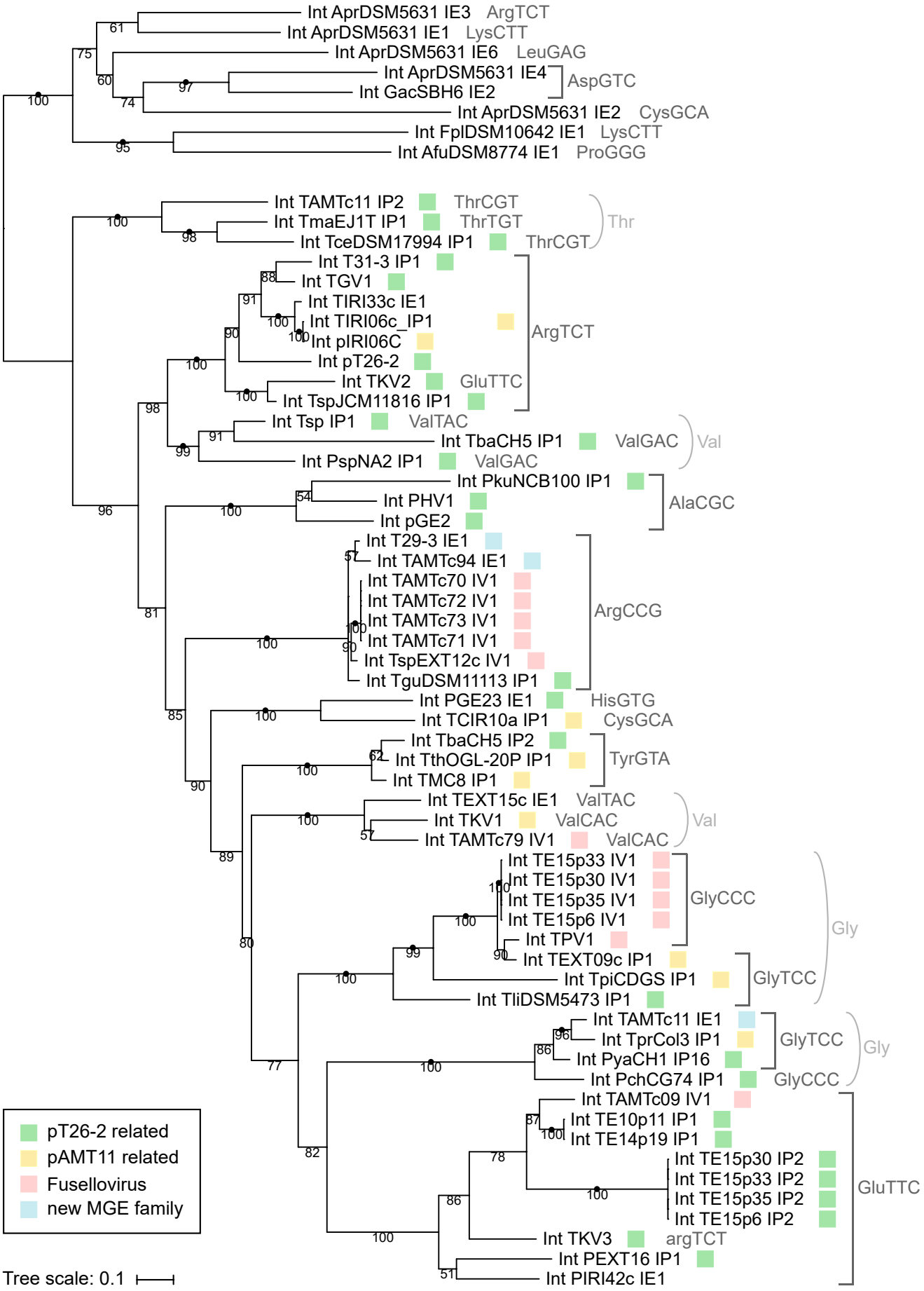

Downloaded from https://academic.oup.com/mbe/advance-article-abstract/doi/10.1093/molbev/msaa041/5739972 by guest on 24 February 2020

Figure 7.

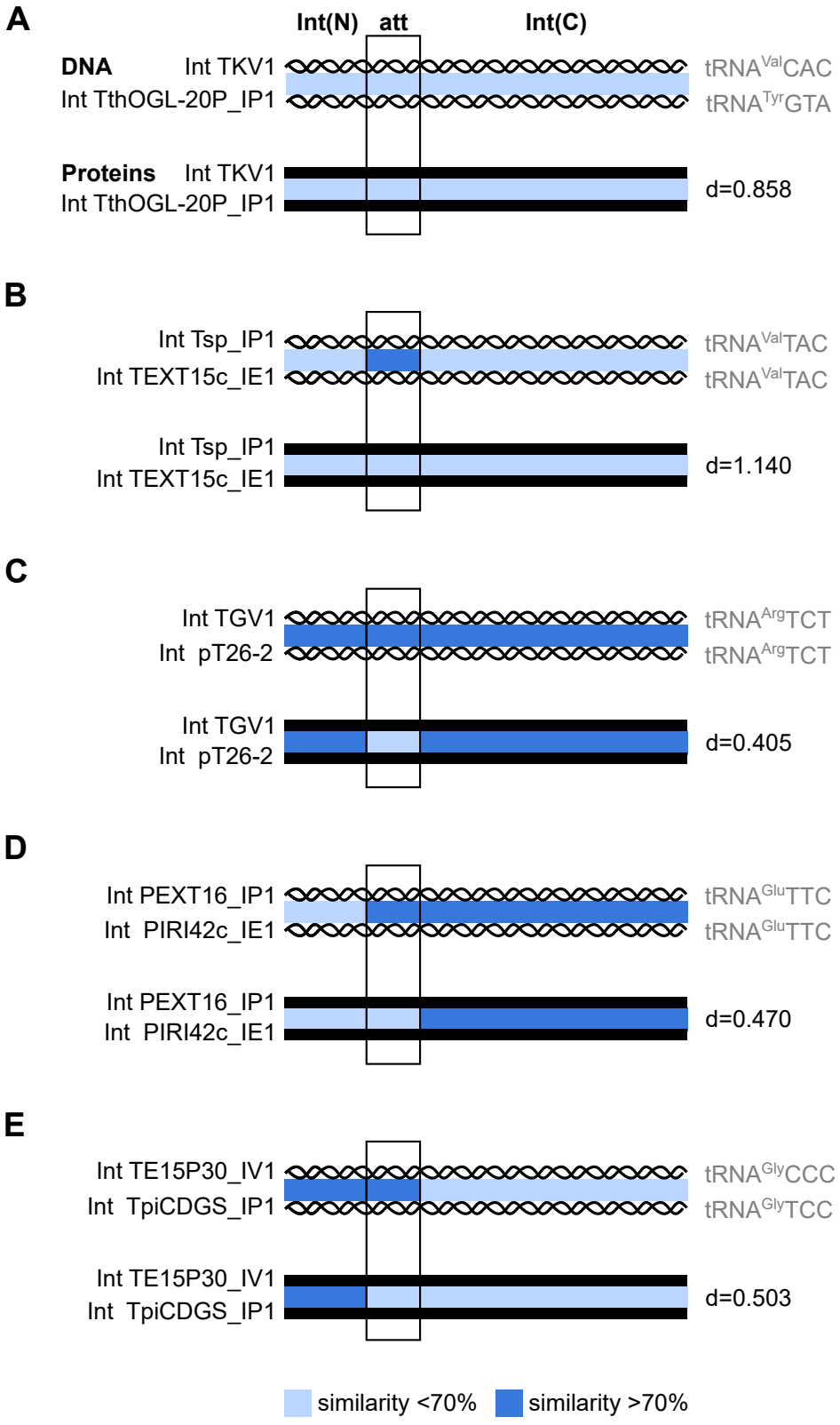

Downloaded from https://academic.oup.com/mbe/advance-article-abstract/doi/10.1093/molbev/msaa041/5739972 by guest on 24 February 2020

Figure 8.

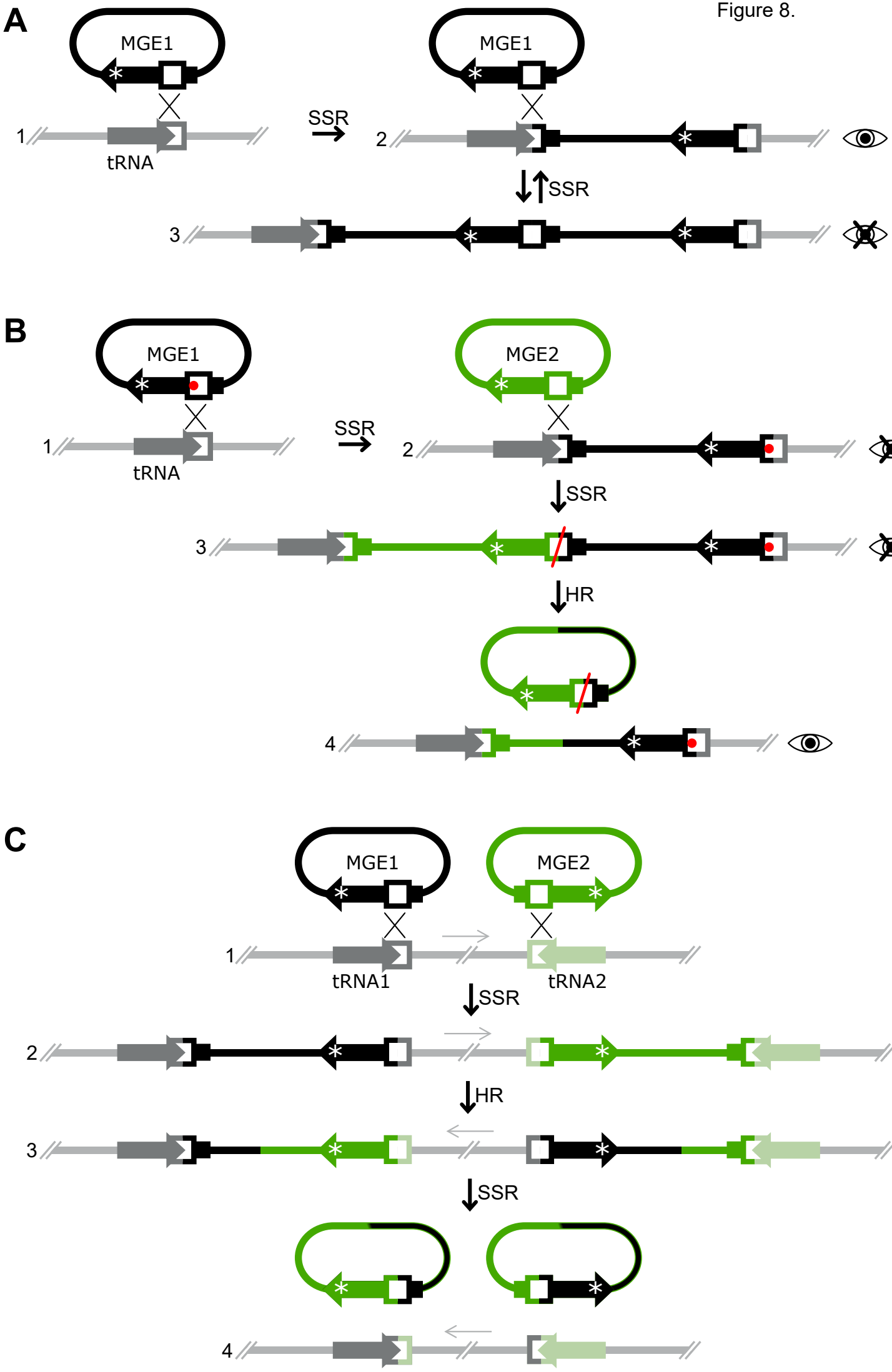

Downloaded from https://academic.oup.com/mbe/advance-article-abstract/doi/10.1093/molbev/msaa041/5739972 by guest on 24 February 2020